SUPPLEMENTAL TABLE 1. **The expression levels of miR-148a, PXR, CYP3A4, HNF4α, and CAR in 25 human livers.**

Sample No.	miR-148a	PXR		CYP3A4		HNF4α	CAR
		mRNA	protein	mRNA	protein	protein	protein
1	1.0	7.7	7.1	1.6	2.6	2.1	2.1
2	9.6	15.2	12.1	201.8	25.0	1.3	1.3
3	3.0	16.6	3.6	38.6	11.5	1.2	1.2
4	7.4	14.1	18.1	61.9	19.5	1.2	1.2
5	6.6	18.7	16.8	248.4	19.7	1.5	1.5
6	6.7	23.4	8.4	3.8	14.5	2.9	2.9
7	2.6	17.8	5.0	8.7	13.2	2.0	2.0
8	7.5	8.6	3.8	1.0	2.6	1.4	1.4
9	2.6	16.6	9.6	74.3	44.9	1.2	1.2
10	2.0	1.0	3.8	2.8	8.3	2.7	2.7
11	3.9	53.0	6.0	10.8	8.7	1.1	1.1
12	10.5	3.6	6.5	3.7	11.5	1.5	1.5
13	8.5	17.7	35.9	208.8	54.6	1.0	1.0
14	21.8	10.2	2.0	5.0	20.1	1.3	1.3
15	25.6	39.6	45.7	77.6	43.4	7.8	7.8
16	62.4	50.5	3.0	185.7	17.3	5.5	5.5
17	38.5	23.5	9.9	362.6	38.4	3.6	3.6
18	19.7	12.8	10.2	169.9	27.9	1.6	1.6
19	14.4	7.8	10.8	37.2	12.4	1.5	1.5
20	32.2	37.6	6.5	284.1	14.6	1.4	1.4
21	27.9	74.9	8.3	338.6	22.9	3.5	3.5
22	11.4	17.9	19.6	172.4	34.6	2.9	2.9
23	94.8	64.8	7.2	44.8	6.3	1.3	1.3
24	12.8	17.3	1.0	59.0	1.0	1.7	1.7
25	23.3	25.0	4.0	67.7	2.9	2.0	2.0

The expression levels of PXR mRNA and CYP3A4 mRNA were determined by real-time RT-PCR and normalized with the GAPDH mRNA level. The expression level of miR-148a was determined by real-time RT-PCR using NCode miRNA First-Strand cDNA Synthesis Kit and was normalized with the U6 snRNA level. The protein levels of PXR, CYP3A4, HNF4α, and CAR were determined by Western blot analyses and normalized with the GAPDH protein level. Data are expressed as relative values in each measurement.

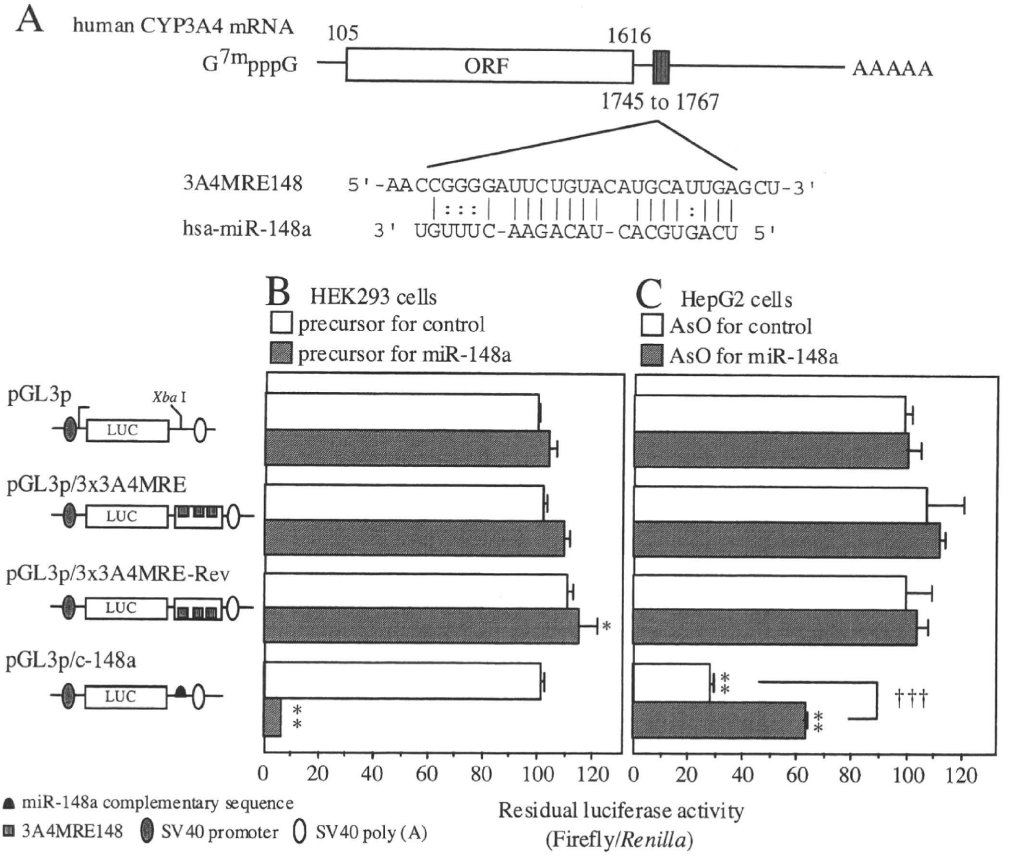

SUPPLEMENTAL FIGURE 1. **CYP3A4 is not directly regulated by miR-148a.** ***A***, Complementarity of miR-148a to the predicted target sequence of CYP3A4. The potential miR-148a recognition element (3A4MRE148) is located on +1745 to +1767 in the 3' UTR of CYP3A4 mRNA, where the numbering refers to the 5' end of mRNA as 1. ***B, C,*** Luciferase assays were performed to investigate whether 3A4MRE148 is functional in the regulation by miR-148a. The reporter constructs were transiently transfected with 4 pmol of the precursors for miR-148a or control into HEK293 cells (***B***) or 10 pmol of the AsO for miR-148a or control into HepG2 cells (***C***). The data were the firefly luciferase activities normalized with the *Renilla* luciferase activities relative to that of pGL3p plasmid. Each column represents the mean ± SD of three independent experiments. $*P < 0.05$, $**P < 0.01$, compared with pGL3p; $\dagger\dagger\dagger P < 0.001$, compared with AsO for control.

Allosteric Kinetics of Human Carboxylesterase 1: Species Differences and Interindividual Variability

SHIORI TAKAHASHI, MIKI KATOH, TAKASHI SAITOH, MIKI NAKAJIMA, TSUYOSHI YOKOI

Drug Metabolism and Toxicology, Division of Pharmaceutical Sciences, Graduate School of Medical Science, Kanazawa University, Kanazawa 920-1192, Japan

Received 29 November 2007; revised 29 January 2008; accepted 4 February 2008

Published online 27 March 2008 in Wiley InterScience (www.interscience.wiley.com). DOI 10.1002/jps.21376

ABSTRACT: Esterified drugs such as imidapril, derapril, and oxybutynin hydrolyzed by carboxylesterase 1 (CES1) are extensively used in clinical practice. The kinetics using the CES1 substrates have not fully clarified, especially concerning species and tissue differences. In the present study, we performed the kinetic analyses in humans and rats in order to clarify these differences. The imidaprilat formation from imidapril exhibited sigmoidal kinetics in human liver microsomes (HLM) and cytosol (HLC) but Michaelis-Menten kinetics in rat liver microsomes and cytosol. The 2-cyclohexyl-2-phenylglycolic acid (CPGA) formation from oxybutynin were not detected in enzyme sources from rats, although HLM showed high activity. The kinetics were clarified to be different among species, tissues, and preparations. In individual HLM and HLC, there was large interindividual variability in imidaprilat (31- and 24-fold) and CPGA formations (15- and 9-fold). Imidaprilat formations exhibited Michaelis-Menten kinetics in HLM and HLC with high activity but sigmoidal kinetics in those with low activity. CPGA formations showed sigmoidal kinetics in high activity HLM but Michaelis-Menten kinetics in HLM with low activity. We revealed that the kinetics were different between individuals. These results could be useful for understanding interindividual variability and for the development of oral prodrugs. © 2008 Wiley-Liss, Inc. and the American Pharmacists Association J Pharm Sci 97:5434–5445, 2008

Keywords: phase I enzyme; prodrugs; enzyme kinetics; phase I metabolism

INTRODUCTION

Carboxylesterase (CES) is one of the phase I drug metabolizing enzymes and is responsible for the hydrolysis of many ester- and amido-type compounds. CES belongs to a serine hydrolase superfamily and is expressed in various mammalian tissues.[1] Mammalian CESs are mainly expressed in liver and small intestine.[2] Recently, human CES was clarified to be expressed in cytosol as well as microsomes in our laboratory.[3] In humans, there are two major isoforms, CES1 and CES2. The human CES1 gene spans approximately 30 kb on chromosome 16q13-q22.1 and has 14 exons.[4] CES1 is mainly expressed in the liver but also in the small intestine at low expression levels.[5] CES1 plays an important role in the metabolism and bioactivation of esterified prodrugs such as capecitabine,[3] imidapril,[6] methylphenidate,[7] and oseltamivir.[8] Esterification is one of the beneficial approaches to increase the oral bioavailability or reduce the adverse reactions of drugs. Therefore, CES1 can be a major

Shiori Takahashi and Miki Katoh contributed equally to this work.

Abbreviations: CES, carboxylesterase; CPGA, 2-cyclohexyl-2-phenylglycolic acid; HLM, human liver microsomes; HLC, human liver cytosol; HJM, human jejunum microsomes; HJC, human jejunum cytosol; RLM, rat liver microsomes; RLC, rat liver cytosol; RJM, rat jejunum microsomes; RJC, rat jejunum cytosol; LC-MS/MS, liquid chromatography-tandem mass spectrometry; BNPP, bis (*p*-nitrophenyl) phosphate; CYP, cytochrome P450; SNP, single nucleotide polymorphism.

Correspondence to: Tsuyoshi Yokoi (Telephone: +81-76-234-4407; Fax: +81-76-234-4407;
E-mail: tyokoi@kenroku.kanazawa-u.ac.jp)

Journal of Pharmaceutical Sciences, Vol. 97, 5434–5445 (2008)
© 2008 Wiley-Liss, Inc. and the American Pharmacists Association

WILEY InterScience® DISCOVER SOMETHING GREAT

determinant of the pharmacological and toxicological effects of prodrugs. Understanding the CES function is necessary to predict the pharmacokinetics of prodrugs. Kinetic analyses are helpful to characterize the enzymatic properties of CES1. The typical CES1 substrates are imidapril, derapril, and oxybutynin, which are clinically used in Japan. Imidapril and derapril are angiotensin-converting enzyme inhibitors and oxybutynin is an anticholinergic drug. Imidapril, derapril, and oxybutynin are hydrolyzed to imidaprilat,[9] deraprilat,[10] and 2-cyclohexyl-2-phenylglycolic acid (CPGA),[11] respectively. In the present study, we selected these three drugs as typical CES1 substrates.

Mammalian CES activities are present in various tissues such as liver, small intestine, lung and blood, and the liver shows the highest hydrolase activity.[12] Some compounds are hydrolyzed by mammalian CESs in microsomes from liver and intestine.[12] In comparison with human CES, there are many isoforms in rats and mice.[12] In addition, as reported by Li et al.,[13] CES was not present in human plasma although it was highly expressed in that of rodents indicating differences in the localization of CES expression between mammalians. Recently, species differences in the pyrethroid hydrolysis reaction have been reported.[14,15] However, sufficient kinetic analyses of the hydrolysis reaction by CES concerning species and tissue differences have not been performed. It is still unclear whether cytosolic CES exhibits similar kinetics to microsomal CES. For drug development, it is important to elucidate the species and tissue differences in CES kinetics. The purpose of the present study was to clarify the kinetics of CES1 hydrolase activity in human liver, human jejunum, rat liver, and rat jejunum. In addition, the differences in microsomal and cytosolic CES1 kinetics were investigated.

MATERIALS AND METHODS

Materials

Imidapril and imidaprilat (a major metabolite of imidapril) were kindly supplied by Tanabe Seiyaku (Osaka, Japan). Derapril was kindly provided by Takeda Pharmaceutical (Osaka, Japan). Oxybutynin, CPGA (a metabolite of oxybutynin), phenytoin, and clonazepam were obtained from Wako Pure Chemicals (Osaka, Japan). Pooled human liver microsomes (pooled HLM), pooled human liver cytosol (pooled HLC), microsomes from 13 individual human livers, and cytosol from 13 individual human livers were purchased from BD Gentest (Woburn, MA). Pooled human jejunum microsomes (pooled HJM) and cytosol (pooled HJC) were obtained from KAC (Shiga, Japan). All other chemicals and solvents were of analytical or the highest grade commercially available.

Preparation of Microsomes and Cytosol from Rat Liver or Jejunum

Wister rats, 7 weeks old, were obtained from Japan SLC, Inc. (Shizuoka, Japan). Pooled microsomes and cytosol from 5 rat livers (RLM and RLC) and jejunums (RJM and RJC) were prepared according to the method of Emoto et al.[16]

Imidaprilat Formation

Imidaprilat formation from imidapril was determined according to the method of Mabuchi et al.[17] with slight modifications. A typical incubation mixture (200 μL of total volume) contained the enzyme source and 100 mM tris(hydroxymethyl)aminomethane-HCl buffer (pH 7.4). After a 2-min preincubation at 37°C, the reaction was initiated by the addition of imidapril and then the mixture was incubated at 37°C for 30 min except for RLM and RLC (10 min). The reaction was terminated by adding 100 μL of ice-cold acetonitrile. After centrifugation at 9000*g* for 5 min, 10 μL of the supernatant were subjected to liquid chromatography-tandem mass spectrometry (LC-MS/MS) system.

LC was performed using an HP 1100 system including a binary pump, an automatic sampler, and a column oven (Agilent Technologies, Waldbronn, Germany), which was equipped with an Inertsil ODS-3 analytical column (2.1 × 100 mm; GL Science, Tokyo, Japan). The column temperature was 40°C and the flow rate was 0.2 mL/min. The mobile phase consisted of acetonitrile/10 mM ammonium formate, 20:80 (v/v). The LC was connected to a PE Sciex API 2000 tandem mass spectrometer (Applied Biosystems, Langen, Germany) operated in the positive electrospray ionization mode. The turbo gas was maintained at 500°C. Nitrogen was used as the nebulizing gas, turbo gas, and curtain gas at 40, 80, and 30 psi, respectively. Parent and/or fragment ions were filtered in the first quadrupole and dissociated in the collision cell using nitrogen as the collision

gas. The collision energy was 27 V. The mass/charge (m/z) ion transitions were recorded in the multiple reaction monitoring mode: m/z 378.2 and 206.3 for imidaprilat. The retention time of imidaprilat was 2.2 min. The limit of detection for imidaprilat was 0.2 pmol. The limit of quantification in the reaction mixture was 20 nM with CV's < 10%. In the preliminary study, a specific CES inhibitor, bis (*p*-nitrophenyl) phosphate (BNPP) (300 μM) inhibited the imidaprilat formation with all enzyme sources at 150 μM imidapril. A CES2 inhibitor, loperamide (20 and 200 μM) did not inhibit the imidaprilat formation in pooled HLM and HLC at 10 and 100 μM imidapril.

Deraprilat Formation

Deraprilat formation from derapril was determined according to the method of Ito et al.[18] with slight modifications. A typical incubation mixture (200 μL of total volume) contained the enzyme source and 100 mM tris(hydroxymethyl)aminomethane-HCl buffer (pH 7.4). Derapril was dissolved in methanol. The final concentration of methanol in the reaction mixture was <1.0%. After a 2-min preincubation at 37°C, the reaction was initiated by the addition of derapril and then the mixture was incubated for 30 min at 37°C. The reaction was terminated by adding 200 μL of ice-cold acetonitrile. Clonazepam (1 nmol) was added as an internal standard. After centrifugation at 9000*g* for 5 min, 50 μL of the supernatant was subjected to high-performance liquid chromatography equipped with a CAPCELL PAK CN UG120 analytical column (4.6 × 150 mm; Shiseido, Tokyo, Japan). The eluent was monitored at 210 nm with a noise-base clean Uni-3 (Union, Gunma, Japan). Deraprilat was quantified using a standard curve of derapril because authentic deraprilat could not be obtained. The column temperature was 35°C and the flow rate was 1.0 mL/min. The mobile phase consisted of acetonitrile/100 mM KH_2PO_4 (pH 3.0), 25:75 (v/v). The retention times of deraprilat and clonazepam were 6.1 and 11.4 min, respectively. In the preliminary study, BNPP (20 μM) inhibited the deraprilat formation with all enzyme sources at 10 μM derapril.

CPGA Formation

CPGA formation from oxybutynin was determined according to the method of Malcolm et al.[19] with slight modifications. A typical incubation mixture (200 μL of total volume) contained the enzyme source and 100 mM potassium phosphate buffer (pH 7.4). After a 2-min preincubation at 37°C, the reaction was initiated by the addition of oxybutynin and then the mixture was incubated for 30 min at 37°C. The reaction was terminated by adding 200 μL of ice-cold acetonitrile. Phenytoin (1 nmol) was added as an internal standard. After centrifugation at 9000*g* for 5 min, 90 μL of the supernatant was subjected to high-performance liquid chromatography equipped with a Develosil C30-UG-5 analytical column (4.6 × 150 mm; Nomura chemical, Aichi, Japan). The eluent was monitored at 220 nm. The column temperature was 35°C and the flow rate was 1.0 mL/min. The mobile phase consisted of acetonitrile/20 mM potassium phosphate buffer (pH 5.0), 40:60 (v/v). The retention times of CPGA and phenytoin were 6.2 and 11.1 min, respectively. The limit of detection for CPGA was 20 pmol. In the preliminary study, BNPP (5 μM) inhibited the CPGA formation with all enzyme sources at 200 μM oxybutynin. Loperamide (20 and 200 μM) did not inhibit the CPGA formation in pooled HLM and HLC at 10 and 100 μM oxybutynin.

Kinetic Analyses of Imidaprilat, Deraprilat, and CPGA Formation

The kinetic analyses were performed using pooled HLM, pooled HLC, RLM, RLC, RJM, and RJC. When the kinetic parameters were determined, the substrate concentrations ranged from 2 to 500 μM for imidapril, from 5 to 1000 μM for derapril, and from 4 to 500 μM for oxybutynin. The imidaprilat formation in HJM and that in HJC were examined at 200 μM imidapril. The protein concentrations of microsomes and cytosol were 0.2 and 1.0 mg/mL, respectively. The protein concentrations of RLM and RLC in the imidaprilat formations were 0.01 and 0.05 mg/mL, respectively. In the preliminary study, the linearity of the protein concentrations and incubation times were confirmed. The kinetic parameters were estimated from the fitted curves using a KaleidaGraph computer program (Synergy, Reading, PA) designed for nonlinear regression analysis. The following equations were used: Michaelis-Menten equation: $V = V_{max} \times [S]/(K_m + [S])$ and Hill equation: $V = (V_{max} \times [S]^n)/(S_{50}^n + [S]^n)$, where V is the velocity of the reaction, S is the substrate

concentration, K_m is the Michaelis-Menten constant, V_{max} is the maximum velocity, S_{50} is the substrate concentration showing the half-V_{max}, and n is Hill coefficient. Intrinsic clearance was calculated as V_{max}/K_m for the Michaelis-Menten kinetics. For the sigmoidal kinetics, the maximum clearance (CL_{max}) was calculated as $V_{max} \times (n-1)/S_{50} \times n(n-1)^{1/n}$ to estimate the highest clearance.[20]

Species and Tissue Differences in CPGA Formation

The CPGA formation was examined at 200 μM oxybutynin in pooled HLM, pooled HLC, pooled HJM, pooled HJC, RLM, RLC, RJM, and RJC. The protein concentrations of microsomes and cytosol were 0.5 and 2.5 mg/mL, respectively.

Interindividual Variability in Imidaprilat and CPGA Formation

Imidaprilat formation and that of CPGA were examined at 20 μM imidapril and 20 μM oxybutynin in 13 HLM and 13 HLC. The protein concentrations of HLM and HLC were 0.2 and 1.0 mg/mL, respectively. For the kinetic analysis of the imidaprilat formation, the individual HLM and HLC that could yield sufficient volumes were used as follows: HLM with high activities (HG3 and HH31), HLM with low activities (HH47 and HG64), HLC with high activities (HH18 and HG89), and HLC with low activities (HH47 and HH31). For the kinetic analysis of the CPGA formation, the individual HLM and HLC were used as follows: HLM and HLC with high activities (HG3 and HH18) and HLM and HLC with low activities (HH47 and HG64).

Statistical Analysis

The correlations between imidaprilat and CPGA formation in individual HLM or HLC were determined by Pearson's product moment method. A p value of less than 0.05 was considered statistically significant.

RESULTS

Kinetic Analysis of Imidaprilat Formation in Human Liver, Rat Liver, and Rat Jejunum

To investigate the differences in the CES1 characteristics between humans and rats or liver and jejunum, kinetic analyses of the imidaprilat formation were carried out in pooled HLM, pooled HLC, RLM, RLC, RJM, and RJC. Kinetic parameters were different between human and rat livers or rat livers and jejunums (Tab. 1). As shown in Figure 1, Eadie-Hofstee plots in pooled HLM and HLC exhibited curved lines at low substrate concentrations although the Hill coefficients were close to 1.0. The apparent S_{50} value in pooled HLM was lower than that of pooled HLC (Tab. 1). The kinetics in RLM and RLC fitted to the Michaelis-Menten equation and the V_{max}/K_m value of RLM was approximately two-fold higher

Table 1. Kinetic Parameters of Imidaprilat Formation in HLM, HLC, RLM, RLC, RJM, and RJC

	High Affinity Isoform			Low Affinity Isoform			
Enzyme Source	K_m (μM)	V_{max} (nmol/min/mg)	V_{max}/K_m (μL/min/mg)	K_m (μM)	V_{max} (nmol/min/mg)	V_{max}/K_m (μL/min/mg)	n
HLM	—	—	—	245[a]	2.4	7.4[b]	1.1 (1.1[c])
HLC	—	—	—	397[a]	0.2	0.5[b]	1.0 (1.1[c])
HJM	—	ND	—	—	—	—	—
HJC	—	ND	—	—	—	—	—
RLM	52	76.6	1459	—	—	—	—
RLC	33	22.4	677	—	—	—	—
RJM	41	1.0	25	346	3.7	10.6	—
RJC	53	0.2	4	382	0.8	2.1	—

n, Hill coefficient calculated using all concentrations of imidapril.
ND; not detected.
[a] S_{50}.
[b] CL_{max}.
[c] Hill coefficient calculated below 100 μM imidapril.

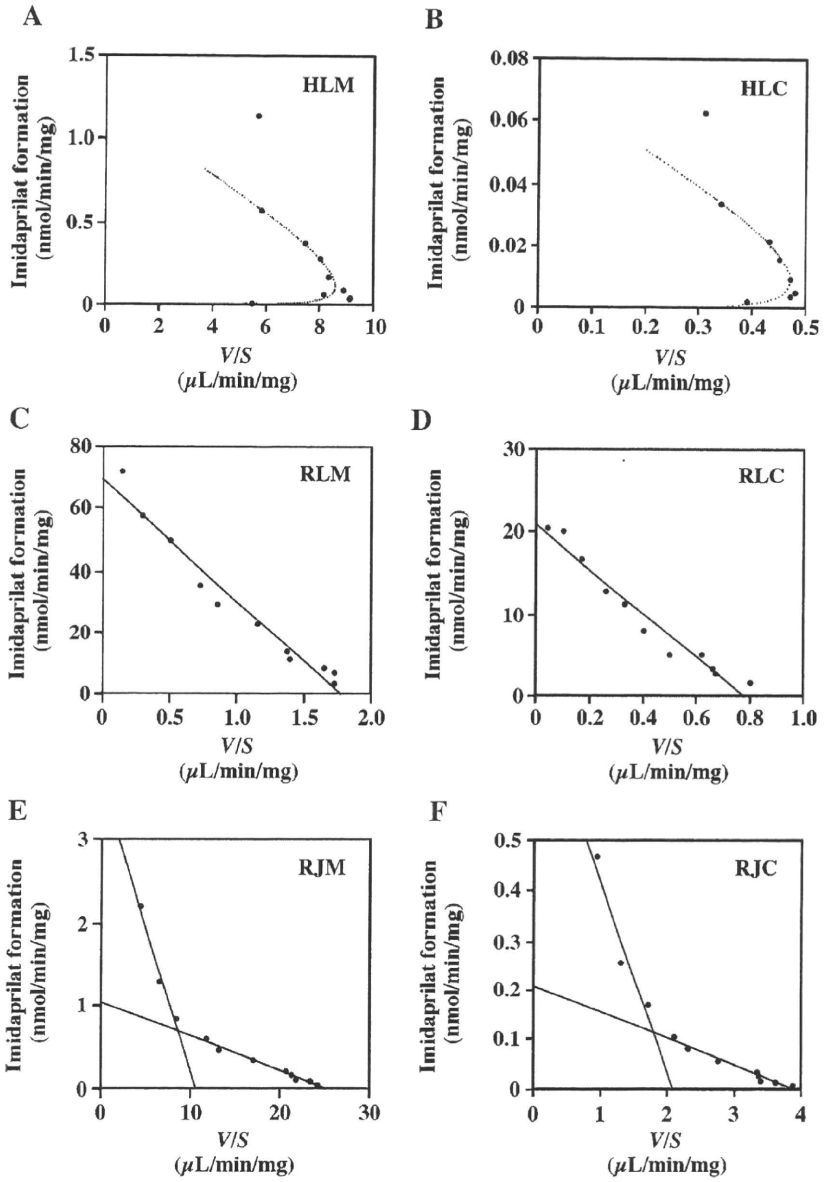

Figure 1. Kinetic analyses of imidaprilat formation catalyzed by pooled HLM (A), pooled HLC (B), RLM (C), RLC (D), RJM (E), and RJC (F). The concentration of imidapril was 2–500 μM. The curved lines (A and B) were estimated by the concentration below 100 μM imidapril. Each data point represents the mean of duplicate determinations.

than that of RLC. RLM and RLC hydrolyzed imidapril more efficiently than pooled HLM and HLC. RJM and RJC appeared bi-phasic in the Eadie-Hofstee plots. The apparent K_m values in RJM and RJC were similar in high and low affinity isoforms, but the V_{max} values of both isoforms in RJM were approximately five-fold higher than those in RJC. Imidaprilat formation in pooled HJM and HJC could not be detected.

Interindividual Variability of Imidaprilat Formation in HLM and HLC

Imidaprilat formation in microsomes from 13 human livers and in cytosol from 13 human livers was determined at 20 μM imidapril (Fig. 2). The interindividual variability of imidaprilat formation in HLM and HLC was 31- and 24-fold, respectively. The imidaprilat formation in HLM

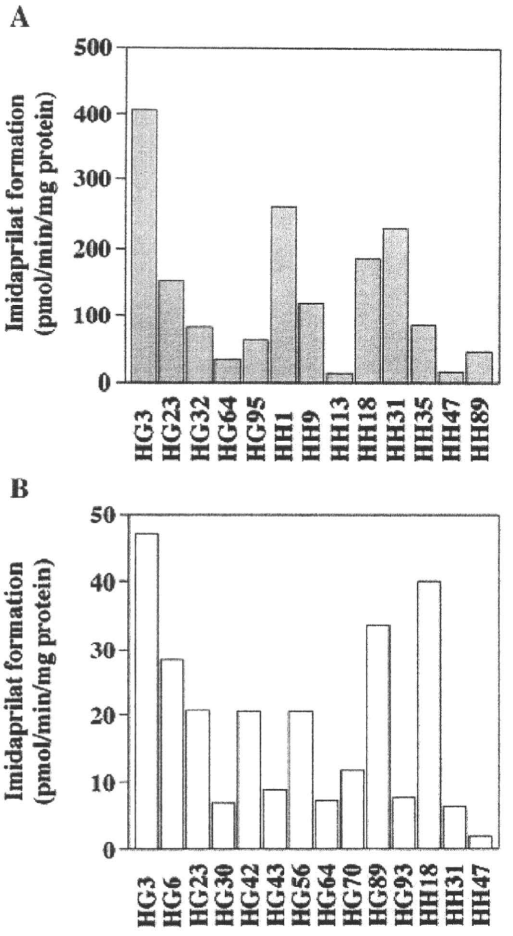

Figure 2. Interindividual variability of imidaprilat formation in 13 HLM (A) and in 13 HLC (B). The concentration of imidapril was 20 μM. Each column represents the mean of duplicate determinations.

ranged from 13.2 pmol/min/mg protein in HH13 to 406.9 pmol/min/mg protein in HG3. On the other hand, the imidaprilat formation in HLC ranged from 2.0 pmol/min/mg protein in HH47 to 47.1 pmol/min/mg protein in HG3. The imidaprilat formation between individual HLM and HLC from the same donors was well-correlated ($n = 6$, $r = 0.77$).

Individual Kinetic Analysis of Imidaprilat Formation in HLM and HLC

Kinetic analyses of the imidaprilat formation were performed in some individual HLM and HLC (Tab. 2). The imidaprilat formation in both HLM and HLC with high activities fitted to the Michaelis-Menten equation, whereas those with low activities fitted curved lines in the Eadie-Hofstee plots (Fig. 3). The K_m values in HLM with high activities were higher than the S_{50} values in HLM with low activities.

Kinetic Analysis of Deraprilat Formation in Human Liver, Rat Liver, and Rat Jejunum

To investigate the effects of structural diversity on the kinetic analysis, kinetic analyses of the deraprilat formation were performed in pooled HLM, pooled HLC, RLM, RLC, RJM, and RJC. The kinetic parameters of the deraprilat formation are shown in Table 3. The Eadie-Hofstee plot of the deraprilat formation was bi-phasic in pooled HLM whereas it was curved in pooled HLC. RLM also appeared bi-phasic in the Eadie-Hofstee plot. The V_{max}/K_m values of high and low affinity isoforms in RLM were higher than those in pooled

Table 2. Kinetic Parameters of Imidaprilat Formation in Individual HLM and HLC

Enzyme Source	Activity	Donor	K_m (μM)	V_{max} (pmol/min/mg)	V_{max}/K_m (μL/min/mg)	n	Model
HLM	High	HG3	119	2310	19.4	—	Michaelis-Menten
		HH31	175	1963	11.2	—	
	Low	HH47	15[a]	48	1.7[b]	1.5 (1.5[c])	Hill
		HG64	84[a]	349	2.9[b]	1.1 (1.1[c])	
HLC	High	HH18	444	905	2.0	—	Michaelis-Menten
		HG89	205	305	1.5	—	
	Low	HH47	420[a]	56	0.1[b]	1.0 (1.2[c])	Hill
		HH31	340[a]	124	0.4[b]	1.0 (1.2[c])	

n, Hill coefficient calculated using all concentrations of imidapril.
[a] S_{50}.
[b] CL_{max}.
[c] Hill coefficient calculated below 100 μM imidapril.

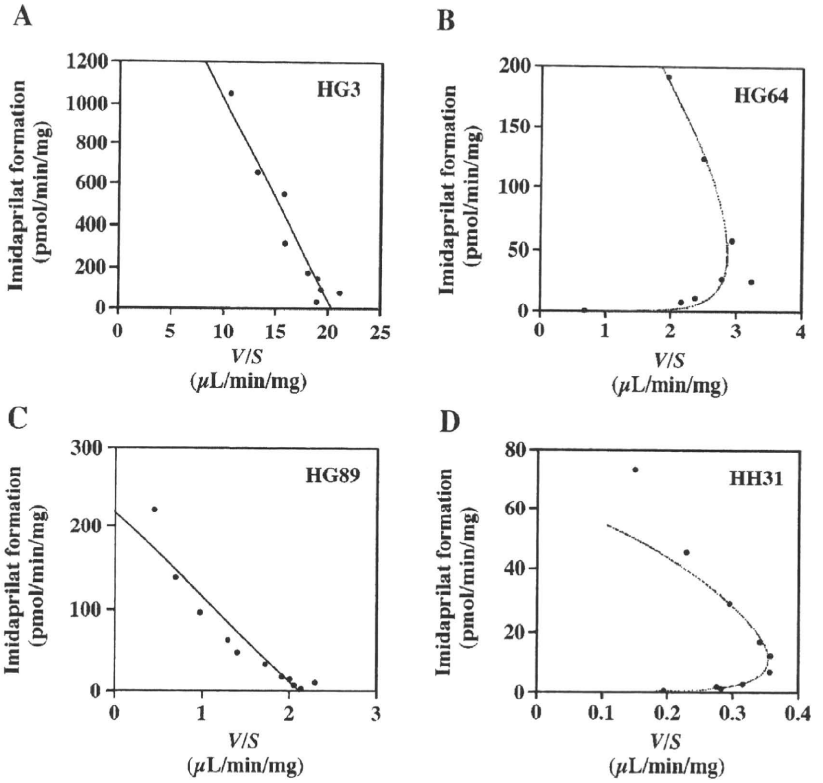

Figure 3. Kinetic analyses of imidaprilat formation catalyzed by individual HLM and HLC. (A) HLM with high activity (HG3); (B) HLM with low activity (HG64); (C) HLC with high activity (HG89); (D) HLC with low activity (HH31). The concentration of imidapril was 2–500 μM. The curved lines (B and D) were estimated by the concentration below 100 μM imidapril. Each point represents the mean of duplicate determinations.

HLM. Eadie-Hofstee plots in RJM and RJC exhibited curved lines at low substrate concentrations ($n = 1.2$). The apparent S_{50} value of RJM was similar to that of RJC, but the CL_{max} value in RJM was higher than that of RJC.

CPGA Formation in Humans and Rats

To clarify the differences of CES1 activity between humans and rats or between liver and jejunum, the CPGA formation was determined at 200 μM

Table 3. Kinetic Parameters of Deraprilat Formation in HLM, HLC, RLM, RLC, RJM, and RJC

	High Affinity Isoform			Low Affinity Isoform			
Enzyme Source	K_m (μM)	V_{max} (nmol/min/mg)	V_{max}/K_m (μL/min/mg)	K_m (μM)	V_{max} (nmol/min/mg)	V_{max}/K_m (μL/min/mg)	n^c
HLM	5.6	1.1	193	460	16.7	36.4	—
HLC	—	—	—	1118[a]	2.8	2.0[b]	1.1
RLM	0.2	0.1	700	33	1.6	49.5	—
RLC	1.7	0.1	29	101	0.8	7.5	—
RJM	—	—	—	28[a]	1.5	32.9[b]	1.2
RJC	—	—	—	41[a]	0.1	1.5[b]	1.2

[a] S_{50}.
[b] CL_{max}.
[c] n, Hill coefficient.

oxybutynin in pooled HLM, pooled HLC, pooled HJM, pooled HJC, RLM, RLC, RJM, and RJC. The pooled HLM showed higher activity (773.5 pmol/min/mg protein) than pooled HLC (38.2 pmol/min/mg protein), pooled HJM (36.8 pmol/min/mg protein), and pooled HJC (5.4 pmol/min/mg protein). No activities were detected in RLM, RLC, RJM, and RJC. Kinetic analyses of the CPGA formation in pooled HLM and HLC were performed and the Eadie-Hofstee plots showed curved lines when the Hill coefficients calculated below 100 μM were 1.5 and 1.1, respectively. As fitted to the Hill equation, the apparent S_{50} values in pooled HLM and HLC were 119.7 and 146.3 μM, respectively and the V_{max} values were 739.1 and 92.4 pmol/min/mg protein, respectively.

Interindividual Variability of CPGA Formation in HLM and HLC

As shown in Figure 2, 15- and 9-fold interindividual variability in the CPGA formation was observed in HLM and HLC, respectively. In HLM, the CPGA formation at 20 μM oxybutynin showed the highest in HG3 (375.3 pmol/min/mg protein) and the lowest in HH47 (25.1 pmol/min/mg protein). In HLC, the CPGA formation showed the highest in HG3 (72.8 pmol/min/mg protein) and the lowest in HG64 (7.6 pmol/min/mg protein) (Fig. 4). The CPGA formation was significantly correlated between individual HLM and HLC from the same donors ($n = 6$, $r = 0.89$, $p < 0.05$). Moreover, the CPGA formation was significantly correlated with the imidaprilat formation in both HLM ($r = 0.98$, $p < 0.001$) and HLC ($r = 0.97$, $p < 0.001$).

Kinetic Analysis of CPGA Formation in Individual HLM and HLC

Kinetic analyses of CPGA formation were performed in individual HLM and HLC (Tab. 4). The apparent K_m values of CPGA formation in HLM and HLC were similar. CPGA formation in HLM and HLC with high activities also exhibited curved lines in the Eadie-Hofstee plots (Fig. 5) and their Hill coefficients calculated below 100 μM showed 1.2 and 1.6, respectively. The Eadie-Hofstee plots in HLM with low activities were monophasic but those in HLC were curved.

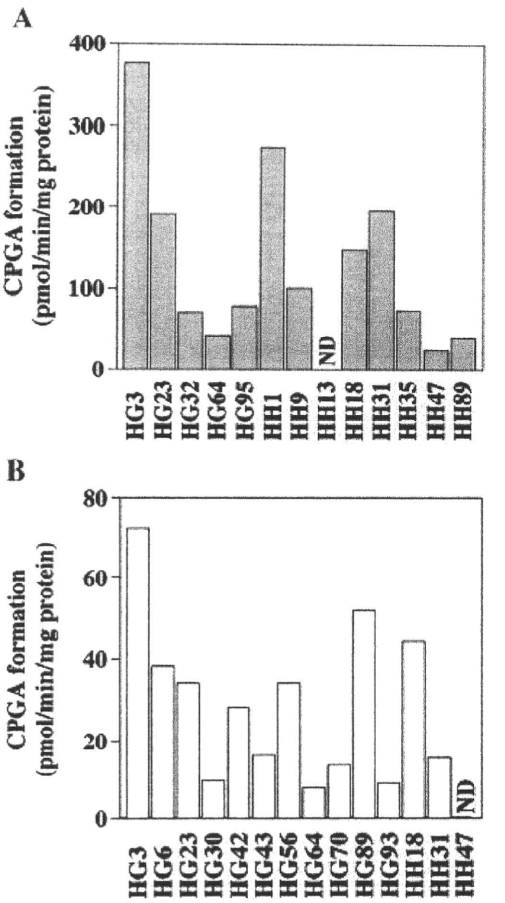

Figure 4. Interindividual variability of CPGA formation in 13 HLM (A) and in 13 HLC (B). The concentration of oxybutynin was 20 μM. Each column represents the mean of duplicate determinations. ND, not detected.

DISCUSSION

It is important to clarify the characteristics of drug metabolizing enzymes for understanding the *in vivo* pharmacokinetics. CES1 is involved in the metabolism of various prodrugs such as imidapril and capecitabine. To investigate the formation of an active metabolite from the prodrug would be important for drug development. However, sufficient information on the enzymatic properties of CES1 is not available. In the preliminary study, the imidaprilat and CPGA formation in HLM and HLC were inhibited by BNPP, but not by loperamide which was a potent CES2 inhibitor,[21] indicating that CES1 would be involved in these hydrolysis. In the present study, kinetic analyses of drugs hydrolyzed by CES1 were performed in humans and rats.

Table 4. Kinetic Parameters of CPGA Formation in Individual HLM and HLC

Enzyme Source	Activity	Donor	K_m (μM)	V_{max} (pmol/min/mg)	V_{max}/K_m (μL/min/mg)	n	Model
HLM	High	HG3	75[a]	1187	10.0[b]	1.2 (1.2[c])	Hill
	Low	HH47	123	107	0.9	—	Michaelis-Menten
HLC	High	HH18	93[a]	283	2.9[b]	1.0 (1.6[c])	Hill
	Low	HG64	94[a]	38	0.3[b]	1.1 (1.5[c])	Hill

n, Hill coefficient calculated using all concentrations of oxybutynin.
[a]S_{50}.
[b]CL_{max}.
[c]Hill coefficient calculated below 100 μM oxybutynin.

In this study, it was first clarified that imidaprilat and CPGA formation showed sigmoidal kinetics in pooled HLM and HLC. The Eadie-Hofstee plots in pooled HLM and HLC were curved sharply at low substrate concentrations (less than 20 μM). The Hill coefficients were estimated to be close to 1.0 when we used all points ranging from 2 to 500 μM imidapril and from 5 to 500 μM oxybutynin. However, the Hill coefficients appeared higher when plotting the activities at only low substrate concentrations. For example, in the CPGA formation in pooled HLM, the Hill coefficient was 1.5 at from 5 to 100 μM oxybutynin. CES1 may behave differently at high substrate concentrations compared with low concentrations. Based on the Eadie-Hofstee plots, it is suggested that CES1 would function allosterically.

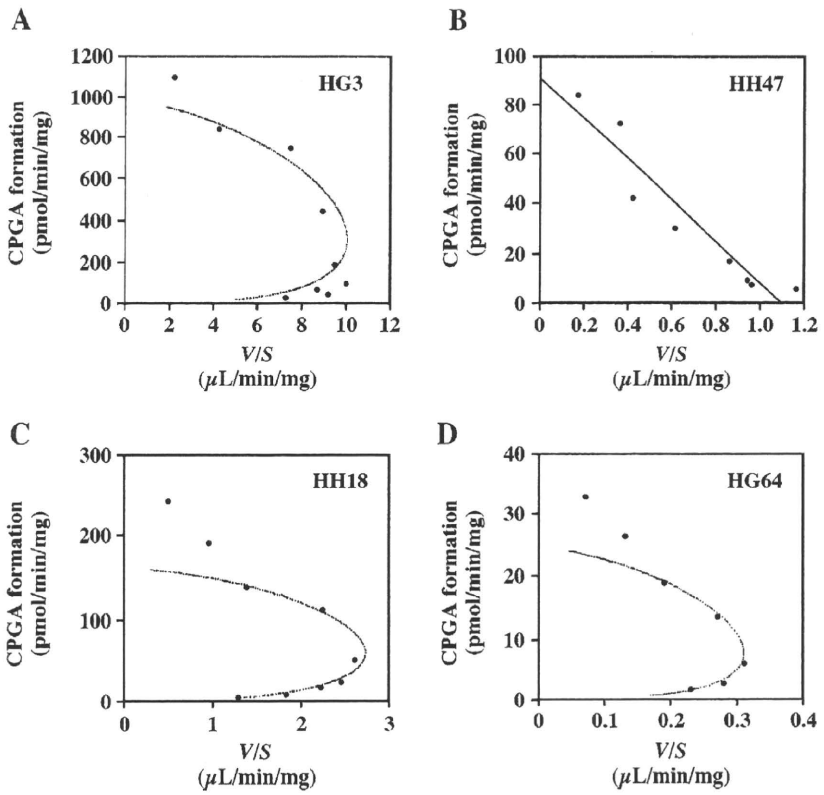

Figure 5. Kinetic analyses of CPGA formation catalyzed by individual HLM and HLC. (A) HLM with high activity (HG3); (B) HLM with low activity (HH47); (C) HLC with high activity (HH18); (D) HLC with low activity (HG64). The concentration of oxybutynin was 4–500 μM. The curved lines (A, C, and D) were estimated by the concentration below 100 μM oxybutynin. Each point represents the mean of duplicate determinations.

Imidaprilat formation in RLM and RLC exhibited Michaelis-Menten kinetics, suggesting that species difference exists. In rat CESs, many isoforms have been identified.[22] In the preliminary study, a specific CES inhibitor, BNPP, inhibited the imidaprilat formation in all enzyme sources from rats. Yamada et al.[23] reported that imidapril was hydrolyzed more efficiently by CES in rat liver than in other tissues. Thus, rat CES should be involved in imidapril metabolism. In the case of another angiotensin-converting enzyme inhibitor, derapril, the kinetics of deraprilat formation in all enzyme sources were different from those of imidaprilat formation. However, derapril has a similar chemical structure to imidapril. Derapril is more bulky than imidapril, thus such a difference might be responsible for the difference in kinetics. On the other hand, no CPGA formation in rats could be detected, suggesting that large species difference would also exist.

In both humans and rats, the V_{max}/K_m or CL_{max} values of the imidaprilat formation in liver were higher than those in jejunum. Human CES1 is mainly expressed in the liver but is found at low expression levels in the small intestine.[24] The differences in the enzymatic activities between liver and jejunum may be explained by the expression levels of CES1. In comparison with microsomes and cytosol in the present study, the V_{max}/K_m or CL_{max} values of imidaprilat formation in all microsomes were higher than those in cytosol. Our previous report indicated that the hydrolysis activity of cytosolic CES1 might be almost equal to that of microsomal CES when taking the protein concentrations into account.[3] Cytosolic proteins are approximately five-fold higher than microsomal proteins in human liver S9.[25] The contribution of cytosolic CES to hydrolysis may be as important as that of microsomal CES in both humans and rats. Recently, human CES1A1 (AB119997) and CES1A2 (AB119998) were registered in GenBank. Their coding regions showed high homology and they had four amino acid differences in their N-terminal regions.[26] Hosokawa et al.[27] speculated that CES1 genes had inverted duplication and were differently regulated at the transcriptional level. However, there are few reports on the differences in the structure, enzymatic activity, and substrate specificity between CES1A1 and CES1A2.

In the present study, there was large interindividual variability in the CES1 activities, which was consistent with previous reports.[3,28] In the imidaprilat formation, the Eadie-Hofstee plot in HLM with low activity was curved sharply around 20 μM, indicating that CES1 may show autoactivation kinetics. The kinetics of imidaprilat formation appeared different depending on the individuals. HLM and HLC with low activity exhibited sigmoidal kinetics in the imidaprilat formation. Since the serum concentration (79 nM) of imidapril in clinical doses (10 mg/day) is lower than the S_{50} value, sigmoidal kinetics may result in the low serum concentration in individuals in comparison with the Michaelis-Menten kinetics. The allosteric effects of CES1 could affect the interindividual variability, but further studies are needed to clarify this issue. There was large interindividual variability in the CPGA formation as in the imidaprilat formation. In individual HLM and HLC, the CPGA formation was significantly correlated with the imidaprilat formation (HLM, $r = 0.98$, $p < 0.001$; HLC, $r = 0.97$, $p < 0.001$), which has been reported to be specifically catalyzed by CES1.[6] Takai et al.[6] also demonstrated that oxybutynin was hydrolyzed by carboxylesterase with pI 4.5, which seems to be CES2, but loperamide did not inhibit the CPGA formation in pooled HLM and HLC in this study. Recombinant CESs are needed to identify the catalytic isoforms, but are not now available. In the present experimental condition, the CPGA formation would be catalyzed by human CES1 because of the significant correlation between the imidaprilat and CPGA formation. In individual HLM and HLC with high activities, the kinetics of the CPGA formation exhibited sigmoidal curves. However, imidaprilat formation in high activity individuals showed Michaelis-Menten kinetics, suggesting that CES1 may behave differently depending on the substrates.

Recently, crystal structures of human CES1 have been reported in complexes with several substrates.[29,30] In such reports, human CES1 contains three ligand binding sites, an active site, a side door, and a Z-site.[31] Bencharit et al.[32] reported that some compounds could bind to the Z-site and that the Z-site may function as an allosteric site, which may be related to the sigmoidal kinetics observed in the present study. Cytochrome P450 3A4 (CYP3A4) has a surface ligand binding site near its active site that may play a role in the recognition of substrates and in the allosteric behavior.[33] The surface ligand binding site of CYP3A4 may correspond to the Z-site of CES1.

Genetic polymorphisms of various drug metabolizing enzymes have been reported and many mutants can affect the catalytic activity.[34] In the case of CYP2B6, the G516T substitution in exon 4 altered the Michaelis-Menten kinetics to sigmoidal kinetics for 7-ethoxycoumarin *O*-deethylase activity.[35] Some single nucleotide polymorphisms (SNPs) can change the kinetic behavior. In the CES1 gene, several SNPs have been identified.[36] Geshi et al.[37] reported that a A(-816)C SNP on the CES1A2 promoter region might affect its transcriptional activity and the elevated responsiveness to imidapril. It is surmised that the genetic polymorphism of CES1 might be responsible for the allosteric effect, but further study is needed to clarify this issue.

In conclusion, species and tissue differences in the CES1 kinetics were elucidated. Moreover, we first clarified that CES1 exhibited sigmoidal kinetics depending on the substrates and the donors of the enzymes. Information on species and tissue differences in CES1 kinetics is important for drug development. For understanding the pharmacokinetics of a CES substrate, we should accumulate basic information concerning the enzyme characteristics. Because the allosteric effects of CES1 may be one of the determinants of the large interindividual variability in clinical doses, the allosteric mechanism should be clarified.

ACKNOWLEDGMENTS

We acknowledge Tanabe Seiyaku for kindly providing imidapril and imidaprilat and Takeda Pharmaceutical for kindly supplying derapril. We thank Mr. Brent Bell for reviewing the manuscript.

REFERENCES

1. Satoh T, Hosokawa M. 2006. Structure, function and regulation of carboxylesterases. Chem Biol Interact 162:195–211.
2. Inoue M, Morikawa M, Tsuboi M, Sugiura M. 1979. Species difference and characterization of intestinal esterase on the hydrolizing activity of ester-type drugs. Jpn J Pharmacol 29:9–16.
3. Tabata T, Katoh M, Tokudome S, Hosokawa M, Chiba K, Nakajima M, Yokoi T. 2004. Bioactivation of capecitabine in human liver: Involvement of the cytosolic enzyme on 5′-deoxy-5-fluorocytidine formation. Drug Metab Dispos 32:762–767.
4. Schaid DJ, McDonnell SK, Wang L, Cunningham JM, Thibodeau SN. 2002. Caution on pedigree haplotype inference with software that assumes linkage equilibrium. Am J Hum Genet 71:992–995.
5. Satoh T, Taylor P, Bosron WF, Sanghani SP, Hosokawa M, LaDu BN. 2002. Current progress on esterases: From molecular structure to function. Drug Metab Dispos 30:488–493.
6. Takai S, Matsuda A, Usami Y, Adachi T, Sugiyama T, Katagiri Y, Tatematsu M, Hirano K. 1997. Hydrolytic profile for ester- or amide-linkage by carboxylesterases pI 5.3 and 4.5 from human liver. Biol Pharm Bull 20:869–873.
7. Sun Z, Murry DJ, Sanghani SP, Davis WI, Kedishvili NY, Zou Q, Hurley TD, Bosron WF. 2004. Methylphenidate is stereoselectively hydrolyzed by human carboxylesterase CES1A1. J Pharmacol Exp Ther 310:469–476.
8. Shi D, Yang J, Yang D, LeCluyse EL, Black C, You L, Akhlaghi F, Yan B. 2006. Anti-influenza prodrug oseltamivir is activated by carboxylesterase human carboxylesterase 1, and the activation is inhibited by antiplatelet agent clopidogrel. J Pharmacol Exp Ther 319:1477–1484.
9. Yamaori S, Fujiyama N, Kushihara M, Funahashi T, Kimura T, Yamamoto I, Sone T, Isobe M, Ohshima T, Matsumura K, Oda M, Watanabe K. 2006. Involvement of human blood arylesterases and liver microsomal carboxylesterases in nafamostat hydrolysis. Drug Metab Pharmacokinet 21: 147–155.
10. Razzetti R, Acerbi D. 1995. Pharmacokinetic and pharmacologic properties of delapril, a lipophilic nonsulfhydryl angiotensin-converting enzyme inhibitor. Am J Cardiol 75:7F–12F.
11. Shinozaki Y, Monden R, Manaka A, Hisa H, Naito S, Igarashi T, Sakai H, Iwata Y, Kasama T. 1986. Studies on metabolic fate of oxybutynin hydrochloride (3) metabolism in human and dog and the site of biotransformation and the effect on enzymes induction in the rats. Xenobio Metabol Dispos 1: 13–24.
12. Satoh T, Hosokawa M. 1998. The mammalian carboxylesterases: From molecules to functions. Annu Rev Pharmacol Toxicol 38:257–288.
13. Li B, Sedlacek M, Manoharan I, Boopathy R, Duysen EG, Masson P, Lockridge O. 2005. Butyrylcholinesterase, paraoxonase, and albumin esterase, but not carboxylesterase, are present in human plasma. Biochem Pharmacol 70:1673–1684.
14. Godin SJ, Scollon EJ, Hughes MF, Potter PM, DeVito MJ, Ross MK. 2006. Species differences in the in vitro metabolism of deltamethrin and esfenvalerate: Differential oxidative and hydrolytic metabolism by humans and rats. Drug Metab Dispos 34:1764–1771.
15. Crow JA, Borazjani A, Potter PM, Ross MK. 2007. Hydrolysis of pyrethroids by human and rat tissues:

Examination of intestinal, liver and serum carboxylesterases. Toxicol Appl Pharmacol 221:1–12.
16. Emoto C, Yamazaki H, Iketaki H, Yamasaki S, Satoh T, Shimizu R, Suzuki S, Shimada N, Nakajima M, Yokoi T. 2001. Cooperativity of alpha-naphthoflavone in cytochrome P450 3A-dependent drug oxidation activities in hepatic and intestinal microsomes from mouse and human. Xenobiotica 31:265–275.
17. Mabuchi M, Kano Y, Fukuyama T, Kondo T. 1999. Determination of imidapril and imidaprilat in human plasma by high-performance liquid chromatography-electrospray ionization tandem mass spectrometry. J Chromatogr B Biomed Sci Appl 734:145–153.
18. Ito H, Yasumatsu M, Usui Y. 1985. Determination of a new angiotensin converting enzyme inhibitor (CV-3317) and its metabolites in serum and urine by high-performance liquid chromatography. Fukuoka Igaku Zasshi 76:441–450.
19. Malcolm K, Woolfson D, Russell J, Tallon P, McAuley L, Craig D. 2003. Influence of silicone elastomer solubility and diffusivity on the in vitro release of drugs from intravaginal rings. J Control Release 90: 217–225.
20. Houston JB, Kenworthy KE. 2000. In vitro-in vivo scaling of CYP kinetic data not consistent with the classical Michaelis-Menten model. Drug Metab Dispos 28:246–254.
21. Quinney SK, Sanghani SP, Davis WI, Hurley TD, Sun Z, Murry DJ, Bosron WF. 2005. Hydrolysis of capecitabine to 5′-deoxy-5-fluorocytidine by human carboxylesterases and inhibition by loperamide. J Pharmacol Exp Ther 313:1011–1016.
22. Mentlein R, Ronai A, Robbi M, Heymann E, von Deimling O. 1987. Genetic identification of rat liver carboxylesterases isolated in different laboratories. Biochim Biophys Acta 913:27–38.
23. Yamada Y, Otsuka M, Takaiti O. 1992. Metabolic fate of the new angiotensin-converting enzyme inhibitor imidapril in animals. 7th communication: In vitro metabolism. Arzneimittelforschung 42: 507–512.
24. Xu G, Zhang W, Ma MK, McLeod HL. 2002. Human carboxylesterase 2 is commonly expressed in tumor tissue and is correlated with activation of irinotecan. Clin Cancer Res 8:2605–2611.
25. Komatsu T, Yamazaki H, Shimada N, Nagayama S, Kawaguchi Y, Nakajima M, Yokoi T. 2001. Involvement of microsomal cytochrome P450 and cytosolic thymidine phosphorylase in 5-fluorouracil formation from tegafur in human liver. Clin Cancer Res 7:675–681.
26. Tanimoto K, Kaneyasu M, Shimokuni T, Hiyama K, Nishiyama M. 2007. Human carboxylesterase 1A2 expressed from carboxylesterase 1A1 and 1A2 genes is a potent predictor of CPT-11 cytotoxicity in vitro. Pharmacogenet Genomics 17:1–10.
27. Hosokawa M, Furihata T, Yaginuma Y, Yamamoto N, Koyano N, Fujii A, Nagahara Y, Satoh T, Chiba K. 2007. Genomic structure and transcriptional regulation of the rat, mouse, and human carboxylesterase genes. Drug Metab Rev 39:1–15.
28. Tang M, Mukundan M, Yang J, Charpentier N, LeCluyse EL, Black C, Yang D, Shi D, Yan B. 2006. Antiplatelet agents aspirin and clopidogrel are hydrolyzed by distinct carboxylesterases, and clopidogrel is transesterificated in the presence of ethyl alcohol. J Pharmacol Exp Ther 319:1467–1476.
29. Bencharit S, Morton CL, Hyatt JL, Kuhn P, Danks MK, Potter PM, Redinbo MR. 2003. Crystal structure of human carboxylesterase 1 complexed with the Alzheimer's drug tacrine: From binding promiscuity to selective inhibition. Chem Biol 10: 341–349.
30. Fleming CD, Bencharit S, Edwards CC, Hyatt JL, Tsurkan L, Bai F, Fraga C, Morton CL, Howard-Williams EL, Potter PM, Redinbo MR. 2005. Structural insights into drug processing by human carboxylesterase 1: Tamoxifen, mevastatin, and inhibition by benzil. J Mol Biol 352:165–177.
31. Bencharit S, Morton CL, Xue Y, Potter PM, Redinbo MR. 2003. Structural basis of heroin and cocaine metabolism by a promiscuous human drug-processing enzyme. Nat Struct Biol 10:349–356.
32. Bencharit S, Edwards CC, Morton CL, Howard-Williams EL, Kuhn P, Potter PM, Redinbo MR. 2006. Multisite promiscuity in the processing of endogenous substrates by human carboxylesterase 1. J Mol Biol 363:201–214.
33. Williams PA, Cosme J, Vinkovic DM, Ward A, Angove HC, Day PJ, Vonrhein C, Tickle IJ, Jhoti H. 2004. Crystal structures of human cytochrome P450 3A4 bound to metyrapone and progesterone. Science 305:683–686.
34. Bosch TM, Meijerman I, Beijnen JH, Schellens JH. 2006. Genetic polymorphisms of drug-metabolising enzymes and drug transporters in the chemotherapeutic treatment of cancer. Clin Pharmacokinet 45:253–285.
35. Ariyoshi N, Miyazaki M, Toide K, Sawamura YI, Kamataki T. 2001. A single nucleotide polymorphism of CYP2B6 found in Japanese enhances catalytic activity by autoactivation. Biochem Biophys Res Commun 281:1256–1260.
36. Marsh S, Xiao M, Yu J, Ahluwalia R, Minton M, Freimuth RR, Kwok PY, McLeod HL. 2004. Pharmacogenomic assessment of carboxylesterases 1 and 2. Genomics 84:661–668.
37. Geshi E, Kimura T, Yoshimura M, Suzuki H, Koba S, Sakai T, Saito T, Koga A, Muramatsu M, Katagiri T. 2005. A single nucleotide polymorphism in the carboxylesterase gene is associated with the responsiveness to imidapril medication and the promoter activity. Hypertens Res 28:719–725.

Chem. Res. Toxicol. **2008,** *21,* 720–725

Human Cytochrome P450 2A13 Efficiently Metabolizes Chemicals in Air Pollutants: Naphthalene, Styrene, and Toluene

Tatsuki Fukami, Miki Katoh, Hiroshi Yamazaki,† Tsuyoshi Yokoi, and Miki Nakajima*

Drug Metabolism and Toxicology, Division of Pharmaceutical Sciences, Graduate School of Medical Science, Kanazawa University, Kakuma-machi, Kanazawa 920-1192, Japan

Human P450 2A13 is the most efficient enzyme for catalyzing the metabolism of nicotine and metabolic activation of 4-(methylnitrosamino)-1-(3-pyridyl)-1-butanone (NNK). It is conceivable that P450 2A13 also metabolizes chemicals in air pollutants because this enzyme is highly expressed in the respiratory tract. In this study, we investigated the possibility that P450 2A13 can metabolize naphthalene, styrene, and toluene, which are included in air pollutants as well as tobacco smoke, although they were known to be metabolized by P450 1A2 or 2E1. We found that P450 2A13 catalyzed 1- and 2-naphthol formations from naphthalene with higher intrinsic clearances (*k*cat/*K*m) (3.1- and 2.2-fold, respectively) than P450 1A2 and also more efficiently catalyzed the styrene 7,8-oxide formation from styrene and the benzylalcohol formation from toluene than P450 2E1. The overlapping substrate specificity of P450 2A13 with P450 2E1 was supported by the finding that P450 2A13 catalyzed chlorzoxazone 6-hydroxylation (8-fold higher value of *k*cat/*K*m) and *p*-nitrophenol 2-hydroxylation (19-fold higher value of *k*cat/*K*m), which are marker activities of P450 2E1. Thus, we found that P450 2A13 metabolizes diverse environmental chemicals and has overlapping substrate specificities of P450 1A2 and 2E1, suggesting that P450 2A13 plays important roles in the local metabolism of environmental chemicals in the respiratory tract related to toxicity or carcinogenicity.

Introduction

The human cytochrome P450 (P450[1]) 2A subfamily comprises three genes: *P450 2A6*, *2A7*, and *2A13* (*1*). Among them, *P450 2A6* and *2A13* encode functional enzymes (*2, 3*). P450 2A13 is the most efficient enzyme in the metabolism of nicotine and metabolic activation of 4-(methylnitrosamino)-1-(3-pyridyl)-1-butanone (NNK) with a substrate specificity similar to that of P450 2A6 (*3, 4*) because of the high amino acid identity between them (93.5%) (*1*). P450 2A6 is predominantly expressed in the liver, whereas P450 2A13 is predominantly expressed in the respiratory tract, with the highest level in the nasal mucosa, followed by the lung and trachea (*3, 5, 6*). P450 2A13 also metabolizes aflatoxin B_1 (*7*). Recently, we found that P450 2A13 can metabolize phenacetin, theophylline (*8*), and 4-aminobiphenyl (*9*), although P450 2A6 showed no or negligible activity. Thus, the substrate specificity of P450 2A13 does not necessarily overlap with that of P450 2A6. Since P450 2A13 is mainly expressed in the respiratory tract, it is feasible that P450 2A13 may catalyze the metabolism of environmental chemicals in air pollutants.

In cigarette smoke, more than 4,000 identified constituents are present. Among them, more than 200 constituents are known to be carcinogens or toxicants. Inhaled cigarette smoke deposits chemicals in the bronchial airway passages and lung. Many carcinogens require activation by enzymes such as P450 to elicit the carcinogenicity or toxicity. Naphthalene is a bicyclic aromatic compound included in cigarette smoke and diesel fumes (*10*). It is also used in the manufacturing of naphthylamines, anthranilic and phthalic acids, and synthetic resins

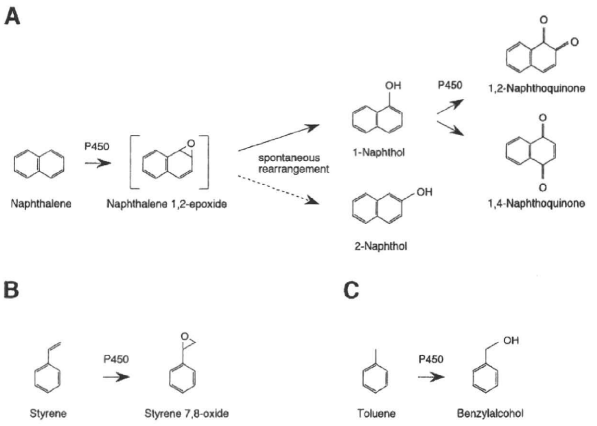

Figure 1. Metabolic pathways of (A) naphthalene, (B) styrene, and (C) toluene by human P450.

(*11, 12*). Naphthalene is mainly converted to 1-naphthol and further to 1,2-naphthoquinone and 1,4-naphthoquinone, the ultimate toxic compounds (Figure 1A). An in vitro study revealed that these naphthoquinones have similar cytotoxicity (*13*). Recently, it has been reported that multiple P450 isoforms are involved in the metabolism of naphthalene and 1-naphthol and that P450 1A2 has the highest activity (*14*). Since the target organs of the toxicity of naphthalene are the lung and bronchus (*15, 16*), and since P450 1A2 is expressed only in the liver, the naphthalene metabolism by the P450 expressed in the respiratory tract should be characterized. Styrene and toluene are widely used as industrial solvents (*17, 18*). High occupational exposure to them results in significant toxicity in the nervous system as well as many organs (*19, 20*). Since they are present in many household products such as aerosols, degreasers, glues, and paints, the general population is likely to be exposed to them. It has been demonstrated that most of the adverse effects of styrene can be attributed to a metabolite, styrene 7,8-oxide (*19*).

* To whom correspondence should be addressed. Tel/Fax: +81-76-234-4407. E-mail: nmiki@kenroku.kanazawa-u.ac.jp.

† Current address: Laboratory of Drug Metabolism and Pharmacokinetics, Shawa Pharmaceutical University, Machida, Tokyo 194-8543, Japan.

[1] Abbreviations: NNK, 4-(methylnitrosamino)-1-(3-pyridyl)-1-butanone; NPR, NADPH-P450 reductase; P450, cytochrome P450.

10.1021/tx700325f CCC: $40.75 © 2008 American Chemical Society
Published on Web 02/12/2008

The epoxidation of styrene is known to be catalyzed by P450 2E1 and 2B6 to a similar extent (Figure 1B) (*21*). The toxicity of toluene is assumed to depend on the duration and magnitude of exposure as well as its metabolic fate. In vitro studies suggested that methyl-hydroxylation by P450 2E1 is a primary detoxification pathway (Figure 1C) (*22, 23*).

In general, the liver is the principal tissue of the metabolism of xenobiotics, but the lung or bronchus that is directly exposed to tobacco carcinogens or air pollutants would also play an important role in the metabolism of xenobiotics. In this study, we investigated whether P450 2A13 has catalytic ability toward naphthalene, styrene, and toluene.

Experimental Procedures

Chemicals. Naphthalene, 1-naphthol, 2-naphthol, styrene, styrene 7,8-oxide, toluene, benzylalcohol, *p*-nitrophenol, and 1,2-dihydroxy-4-nitrobenzene were from Wako Pure Chemicals (Osaka, Japan). Chlorzoxazone and 6-hydroxychlorzoxazone were from Sigma-Aldrich (St. Louis, MO). $NADP^+$, glucose-6-phosphate, and glucose-6-phosphate dehydrogenase were purchased from Oriental Yeast (Tokyo, Japan). All other chemicals and solvents were of the highest or analytical grade commercially available.

Enzyme Preparations. *Escherichia coli* (*E. coli*) membranes expressing recombinant human P450/NADPH-P450 reductase (NPR) for P450 1A1 (*24*), 1A2 (*24*), 2A6 (*25*), 2A13 (*26*), and 2E1 (*24*) were prepared as described previously (*25*). The P450 content (*27*) and protein concentration (*28*) were determined according to a method described previously. The NADPH-cytochrome *c* reductase activity was determined as described previously (*29, 30*) using $\Delta_{\varepsilon 550} = 21.1\ mM^{-1}\ cm^{-1}$, and the content was calculated using the specific activity of 3.0 μmol reduced cytochrome *c*/min/nmol NPR based on purified rabbit NPR preparation (*31*). The molar ratios of NPR to P450 were 3.0 (P450 1A1), 0.8 (P450 1A2), 5.8 (P450 2A6), 2.9 (P450 2A13), and 1.3 (P450 2E1), which were sufficiently high to measure the activities as reported previously (*24*).

Enzyme Assays for Naphthalene Hydroxylation and Naphthoquinone Formation from 1-Naphthol. 1- Naphthol and 2-naphthol formation from naphthalene was determined as follows: A typical incubation mixture (0.2 mL total volume) contained an *E. coli* membrane preparation (3 pmol of P450), 100 mM potassium phosphate buffer (pH 7.4), an NADPH-generating system (0.5 mM $NADP^+$, 5 mM glucose-6-phosphate, 5 mM $MgCl_2$, and 1 U/mL glucose-6-phosphate dehydrogenase) and 5–200 μM naphthalene. The reaction was initiated by the addition of the NADPH-generating system after 2-min preincubation at 37 °C. After 5 min of incubation at 37 °C, the reaction was terminated by the addition of 100 μL of cold acetonitrile. After the removal of the protein by centrifugation at 6,500*g* for 5 min, a 20 μL portion of the supernatant was subjected to HPLC. HPLC analyses were performed using an L-7100 pump (Hitachi, Tokyo, Japan), an L-7200 autosampler (Hitachi), and a D-2500 integrator (Hitachi) equipped with a Mightysil RP-18 C18 GP (4.6 × 150 mm; 5 μm) column (Kanto Chemical, Tokyo, Japan). The eluent was monitored at 223 nm with a noise-base clean Uni-3 (Union, Gunma, Japan), which can reduce the noise by integrating the output and increase the signal 3-fold by differentiating the output and 5-fold by further amplification with an internal amplifer, resulting in a maximum 15-fold amplification of the signal. The mobile phase was 30% acetonitrile containing 0.01% phosphoric acid. The flow rate was 1.0 mL/min. The column temperature was 35 °C. The quantification of 1-naphthol and 2-naphthol was performed by comparing the HPLC peak heights with those of authentic standards.

1,2-Naphthoquinone and 1,4-naphthoquinone formation from 1-naphthol was also determined. A typical incubation mixture, reaction condition, and HPLC condition were the same as described above except that 5–200 μM 1-naphthol was added as a substrate, and a 50 μL portion of the supernatant was subjected to HPLC. Once formed, 1,2-naphthoquinone and 1,4-naphthoquinone were effectively reduced by NPR in the membrane of the *E. coli* expression systems. Therefore, instead of the direct estimation with the HPLC peak heights of 1,2-naphthoquinone and 1,4-naphthoquinone, the disappearance of the peak height of the substrate was calculated for the estimation of 1,2-naphthoquinone and 1,4-naphthoquinone formation.

Enzyme Assay for Styrene 7,8-Epoxidation. Styrene 7,8-oxide formation from styrene was determined as follows: a typical incubation mixture (final volume of 0.2 mL) contained an *E. coli* membrane preparation (5 pmol of P450), 100 mM Tris-HCl buffer (pH 7.4), the NADPH-generating system, and 20–1000 μM styrene. The reaction was initiated by the addition of the NADPH-generating system after 2 min of preincubation at 37 °C. After 10 min of incubation at 37 °C, the reaction was terminated by the addition of 10 μL of 60% perchloric acid. After the removal of protein by centrifugation at 9,500*g* for 5 min, a 60 μL portion of the supernatant was subjected to HPLC. The HPLC apparatus was the same as that described above, except for a Capcell Pak C18 UG120 (4.6 × 150 mm, 5 μm) column (Shiseido, Tokyo, Japan). The eluent was monitored at 200 nm with a noise-base clean Uni-3. The mobile phase was 8% acetonitrile containing 0.25% phosphoric acid. The flow rate was 1.0 mL/min. The column temperature was 35 °C. The quantification of styrene 7,8-oxide was performed by comparing the HPLC peak height with that of an authentic standard.

Enzyme Assay for Toluene methyl Hydroxylation. Benzylalcohol formation from toluene was determined as follows: a typical incubation mixture (final volume of 0.2 mL) contained an *E. coli* membrane preparation (5 pmol of P450), 100 mM Tris-HCl buffer (pH 7.4), the NADPH-generating system, and 50–2000 μM toluene. The reaction was initiated by the addition of the NADPH-generating system after 2 min of preincubation at 37 °C. After 5 min of incubation at 37 °C, the reaction was terminated by the addition of 10 μL of 60% perchloric acid. After the removal of protein by centrifugation at 9,500*g* for 5 min, a 60 μL portion of the supernatant was subjected to HPLC. The HPLC apparatus was the same as that described above, except for a Capcell Pak C18 UG120 (4.6 × 250 mm, 5 μm) column. The eluent was monitored at 200 nm with a noise-base clean Uni-3. The mobile phase was 7% acetonitrile containing 0.1% phosphoric acid. The flow rate was 1.0 mL/min. The column temperature was 35 °C. The quantification of benzylalcohol was performed by comparing the HPLC peak height with that of an authentic standard.

Other Enzyme Assays. Chlorzoxazone 6-hydroxylation was determined as described previously (*32*). *p*-Nitrophenol 2-hydroxylation was also determined as described previously (*33*), except that 100 mM potassium phosphate buffer (pH 7.4) was used.

Statistical Analysis. Statistical analyses of the kinetic parameters were performed by two-tailed Student's *t*-test. A value of $P < 0.05$ was considered statistically significant.

Results

Naphthalene Hydroxylation and Naphthoquinone Formation from 1-Naphthol. The catalytic activities of P450 2A13 for 1-naphthol and 2-naphthol formation from naphthalene were measured by comparing them with those of P450 1A1, 1A2, and 2A6. Naphthalene was predominantly converted to 1-naphthol rather than 2-naphthol, in agreement with a previous report (*14*). As shown in Figure 2A and B, P450 2A13 showed the highest activities for these formations. The activities catalyzed by P450 2A6 were similar to those by P450 1A2. P450 1A1 showed the lowest 1-naphthol formation and no 2-naphthol formation. The kinetic parameters of these reactions are summarized in Table 1. For the 1-naphthol formation, the *K*m value of P450 2A13 was similar to those of P450 1A2 and P450 2A6, and the value of P450 1A1 was prominently high. The *V*max value of P450 2A13 was the highest of all four isoforms. Thus, P450 2A13 showed the highest intrinsic clearance. For the 2-naphthol formation, the *K*m value of P450 2A13 was similar

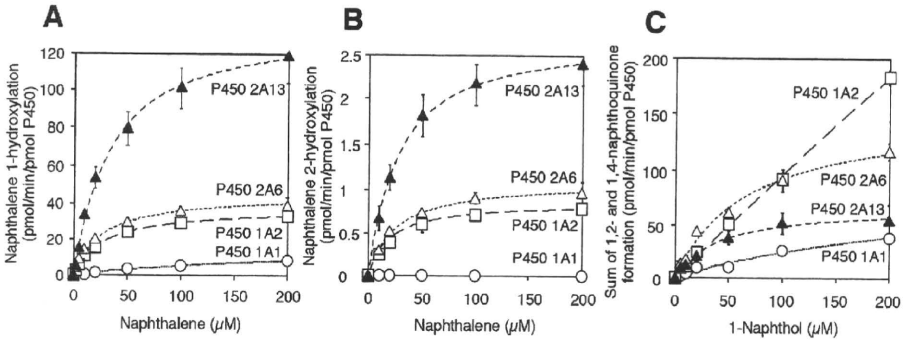

Figure 2. Kinetic analyses of (A) 1-naphthol and (B) 2-naphthol formation from naphthalene, and (C) the total formation of 1,2-naphthoquinone and 1,4-naphthoquinone from 1-naphthol catalyzed by recombinant P450 1A1, 1A2, 2A6, and 2A13 expressed in *E. coli*. The kinetic parameters were estimated from the fitted curve using the computer program KaleidaGraph designed for nonlinear regression analysis. Each data point represents the mean of triplicate determinations.

Table 1. Kinetic Parameters for 1-Naphthol and 2-Naphthol Formation from Naphthalene[a]

	*K*m (μM)	*k*cat (min^{-1})	*k*cat/*K*m (min^{-1} μM^{-1})
	1-naphthol formation from naphthalene		
P450 1A1	244 ± 45[d]	17 ± 1[d]	0.07 ± 0.01[d]
P450 1A2	29 ± 1	39 ± 1	1.34 ± 0.02
P450 2A6	23 ± 4[c]	43 ± 5	1.90 ± 0.16[d]
P450 2A13	36 ± 2[c]	143 ± 15[d]	4.03 ± 0.58[d]
	2-naphthol formation from naphthalene		
P450 1A1	ND[b]	ND	ND
P450 1A2	19.1 ± 2.5	0.9 ± 0.0	0.05 ± 0.01
P450 2A6	26.5 ± 5.2	1.2 ± 0.1[c]	0.05 ± 0.01
P450 2A13	28.2 ± 2.4[c]	2.9 ± 0.4[d]	0.10 ± 0.00[d]

[a] Data are the mean ± SD of three independent experiments. [b] ND, not detected. [c] $P < 0.05$. [d] $P < 0.005$ compared with P450 1A2.

to that of P450 2A6, but higher than that of P450 1A2. The *V*max value of P450 2A13 was higher than those of P450 1A2 and 2A6. Thus, P450 2A13 showed the highest intrinsic clearance.

The total metabolism of 1-naphthol to 1,2-naphthoquinone plus 1,4-naphthoquinone was determined (Figure 2C), and therefore, the kinetic parameters were not calculated. When the total formation of 1,2-naphthoquinone and 1,4-naphthoquinone by the four P450 isoforms was compared, P450 2A6 showed the highest activity at low substrate concentrations (5–20 μM), but P450 1A2 showed the highest activity at the high substrate concentration (200 μM). At the substrate concentrations of 5–50 μM, P450 2A13 showed activity similar to that of P450 1A2. P450 1A1 showed the lowest activity. Collectively, these results suggested that P450 2A13 has the highest catalytic activity for naphthalene and subsequent 1-naphthol metabolisms.

Styrene 7,8-Epoxidation. The catalytic activity of P450 2A13 for styrene 7,8-oxide formation from styrene was measured by comparing it with those of P450 2E1 and 2A6. As shown in Figure 3A, the activities catalyzed by the three P450s were increased in a substrate concentration-dependent manner. The maximum substrate concentration (1 mM) was not sufficiently high to determine the *K*m values because the solubility of styrene limited the substrate concentration that could be achieved in the incubation mixture. Therefore, the *CL*int values were calculated with the initial slope of the plots of velocity versus substrate concentration. The values in P450 2A13, 2A6, and 2E1 were 46.8, 17.2, and 18.5 min^{-1} mM^{-1}, respectively. These results suggest that P450 2A13 has the highest catalytic activity for styrene 7,8-oxide formation from styrene.

Toluene Methyl Hydroxylation. The catalytic activity of P450 2A13 for benzylalcohol formation from toluene was measured by comparing it with those of P450 2E1 and 2A6. As shown in Figure 3B, the activities catalyzed by the three P450s were increased in a substrate concentration-dependent manner. The maximum substrate concentration (2 mM) was not sufficiently high to determine the *K*m values because the solubility of toluene limited the substrate concentration that could be achieved in the incubation mixture. Thus, accurate kinetic parameters could not be obtained. The *CL*int values calculated with the initial slope of the plots of velocity versus substrate concentration in P450 2A13, 2A6, and 2E1 were 13.3, 2.6, and 5.7 min^{-1} mM^{-1}, respectively. These results suggest that P450 2A13 has the highest catalytic activity for benzylalcohol formation from toluene.

Chlorzoxazone 6-Hydroxylation and *p*-Nitrophenol 2-Hydroxylation. The results of our study prompted us to investigate the possibility that the substrate specificity of P450 2A13 might overlap with that of P450 2E1. The chlorzoxazone 6-hydroxylation and *p*-nitrophenol 2-hydroxylation, which are marker activities of P450 2E1, were measured using recombinant P450 2A13, 2A6, and 2E1. Interestingly, P450 2A13 showed significantly higher catalytic activities for both chlorzoxazone 6-hydroxylation and *p*-nitrophenol 2-hydroxylation than P450 2E1 (Figure 4A and B). As shown in Table 2, the *K*m value for chlorzoxazone 6-hydroxylation by P450 2A13 was approximately one-eighth of that by P450 2E1, and their *V*max values were similar, resulting in 8-fold higher intrinsic clearance than that by P450 2E1. P450 2A6 also catalyzed the chlorzoxazone 6-hydroxylation, but the intrinsic clearance was one-fifth of that by P450 2E1. P450 2A13 catalyzed *p*-nitrophenol 2-hydroxylation with significantly higher (19-fold) intrinsic clearances than that by P450 2E1 (Figure 4B and Table 2) and with a lower *K*m value and higher *V*max value than those of P450 2E1. P450 2A6 also catalyzed the *p*-nitrophenol 2-hydroxylation with clearance similar to that by P450 2E1. These results suggest that P450 2A13 can catalyze the metabolism of P450 2E1 substrates.

Discussion

In the present study, we found that P450 2A13 is catalytically active toward chemicals in air pollutants. P450 2A13 showed significantly higher intrinsic clearances for naphthalene hydroxylation than P450 1A2. Recently, we reported that P450 2A13 is catalytically active toward substrates of P450 1A2, such as aminobiphenyl (*9*), theophylline, and phenacetin (*8*). Especially, it was noteworthy that the catalytic activity of P450 2A13 for phenacetin *O*-de-ethylation was apparently higher than that of P450 1A2. On the basis of the present results, naphthalene

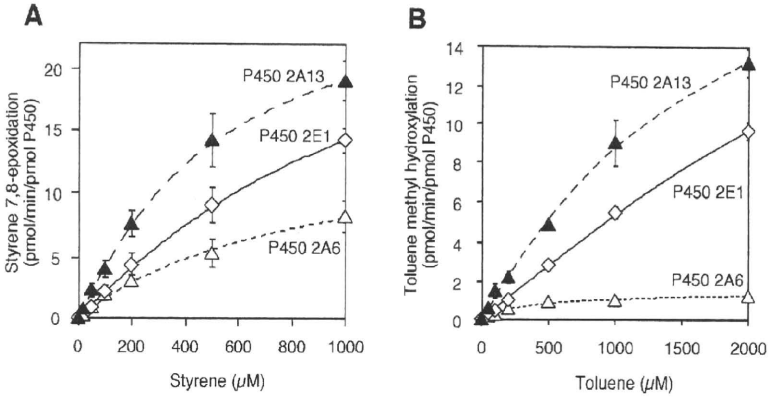

Figure 3. Kinetic analyses of (A) styrene 7,8-oxide formation from styrene and (B) benzylalcohol formation from toluene catalyzed by recombinant P450 2A6, 2A13, and 2E1 expressed in *E. coli*. The styrene and toluene concentrations ranged from 20 to 1000 μM and from 50 to 2000 μM, respectively. Each data point represents the mean of triplicate determinations.

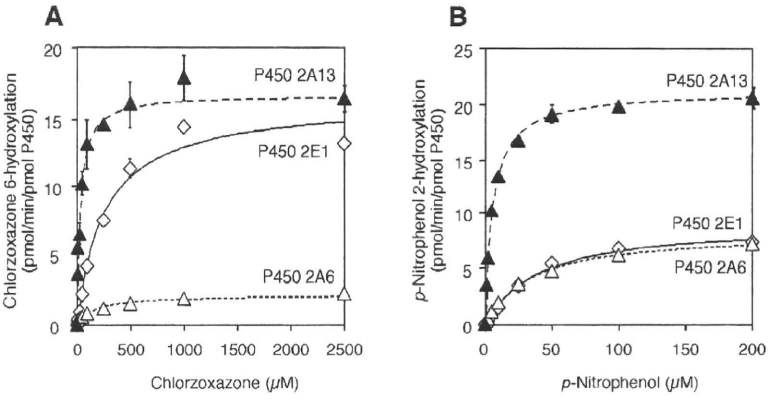

Figure 4. Kinetic analyses of (A) chlorzoxazone 6-hydroxylation and (B) *p*-nitrophenol 2-hydroxylation catalyzed by recombinant P450 2A6, 2A13, and 2E1 expressed in *E. coli*. The kinetic parameters were estimated from the fitted curve using the computer program KaleidaGraph designed for nonlinear regression analysis. Each data point represents the mean of triplicate determinations.

Table 2. Kinetic Parameters for Chlorzoxazone 6-Hydroxylation and *p*-Nitrophenol 2-Hydroxylation[a]

	Km (μM)	kcat (min^{-1})	kcat/Km (min^{-1} μM^{-1})
	chlorzoxazone 6-hydroxylation		
P450 2E1	274 ± 18	16.2 ± 0.3	0.06 ± 0.00
P450 2A6	161 ± 19[c]	2.0 ± 0.2[c]	0.01 ± 0.00[c]
P450 2A13	36 ± 4[c]	16.9 ± 1.3	0.47 ± 0.02[c]
	p-nitrophenol 2-hydroxylation		
P450 2E1	39.6 ± 0.2	9.1 ± 0.1	0.20 ± 0.00
P450 2A6	30.9 ± 1.9[c]	8.4 ± 0.3[b]	0.27 ± 0.06[b]
P450 2A13	5.5 ± 0.1[c]	20.4 ± 0.6[c]	3.73 ± 0.06[c]

[a] Data are the mean ± SD of three independent experiments. [b] $P < 0.05$. [c] $P < 0.005$ compared with P450 2E1.

can be added to the P450 2A13 substrates with overlapping substrate specificity with P450 1A2. P450 2A6 also catalyzed naphthalene hydroxylation with similar or higher intrinsic clearance than P450 1A2. A previous study reported that 1-naphthol and 2-naphthol formation from naphthalene in human liver microsomes was inhibited by antibodies toward p450 2a5, mouse orthologue of P450 2A6, to 50–60% and 30–40% of control, respectively (*34*). In addition, Asikainen et al. reported that coumarin 7-hydroxylation in human liver microsomes, a marker activity of P450 2A6, was inhibited by naphthalene in a competitive manner ($K_i = 1.2 - 5.6$ μM) (*34*). Supporting the study, we directly demonstrated that P450 2A6 catalyzes naphthalene hydroxylation.

We found that P450 2A13 showed higher activity for styrene 7,8-oxide formation from styrene than P450 2E1. Styrene 7,8-oxide, which is classified in group 2A (probably carcinogenic to humans) (*18*), is a major reactive metabolite of styrene, and its genotoxicity has been demonstrated by several in vitro test systems (*35, 36*). P450 2A13 also showed higher activity for benzylalcohol formation from toluene, a major detoxification pathway. Toluene is known to be mainly metabolized by P450 2E1. These results suggest that P450 2A13 is active in the metabolism of the P450 2E1 substrates, supported by the fact that P450 2A13 can catalyze chlorzoxazone 6-hydroxylation and *p*-nitrophenol 2-hydroxylation. The bicistronic P450/NPR *E. coli* membranes used in the present study do not include cytochrome b_5. Since it has been reported that the P450 2E1 activity was enhanced by cytochrome b_5 (*24*), we performed a preliminary study to compare the activities of P450 2E1 and 2A13 in the presence of cytochrome b_5. When cytochrome b_5 expressed in *E. coli* was added with equal molar concentration to P450, chlorzoxazone 6-hydroxymation (30 μM substrate concentration) and *p*-nitrophenol 2-hydroxylation (5 μM substrate concentration) catalyzed by P450 2E1 were increased by approximately 2-fold, but these were still considerably (one forth) lower than the activities catalyzed by P450 2A13 in the absence of cytochrome b_5 (Figure S1, Supporting Information). The effects of cytochrome b_5 on styrene 7,8-oxide formation from styrene and benzylalcohol formation from toluene by P450 2E1 and 2A13 were trivial (Figure S1, Supporting Information). Thus, our findings that P450 2A13 showed higher activities toward styrene, toluene, chlorzoxazone, and *p*-nitrophenol were not reversed in the presence of cytochrome b_5. It is generally accepted that P450 2E1 metabolizes a variety of toxins and carcinogens included in air pollutants, such as benzene, xylene,

acrylonitrile, and ethylcarbamate (urethane) (*37*). Therefore, it would be interesting to investigate whether P450 2A13 can catalyze the metabolism of such chemicals in the future.

Recently, Smith et al. (*38*) determined the structure of P450 2A13 by X-ray crystallography and compared it with the structure of P450 2A6. They reported that the overall P450 2A13 and 2A6 structures are very similar. Like 2A6, the P450 2A13 active site is small, planar, and highly hydrophobic with a cluster of phenylalanine residues for $\pi-\pi$ interactions with aromatic ligands. Sansen et al. (*39*) reported that the active site of P450 1A2 is also relatively small and narrow throughout its extent. The X-ray crystallography of P450 2E1 has not yet accomplished, but it is easily assumed that the P450 2E1 active site is relatively small because its substrate molecules are typically small (molecular weight <100). Smith et al. (*38*) reported that the differences in residues 117, 208, 300, and 301 (for definition of the plane of ligands), and residues 365 and/or 366 (for determination of the ligand binding and catalysis) in the active site may be accountable for the difference of substrate specificity between P450 2A13 and 2A6. We cannot compare the residues at comparable sites in P450 1A2 and 2E1 since the overall structures of P450 1A2 and 2E1 are likely to show considerable changes from those of P450 2A6 and 2A13. However, the relative size and planarity of the P450 1A2 active site compared to that of P450 2A13 have some bearing on overlapping substrate specificity.

Naphthalene, styrene and toluene are included in environmental air as hazardous solvents in many industrial workshops and homes. Because they are easily absorbed by inhalation, their local metabolism in the respiratory tract may be as important as that in the liver. P450 2A13 is predominantly expressed in the respiratory tract such as in the lung and trachea (*3, 5*). Recently, the expression of P450 2A13 protein in the epithelia of the bronchus and lung was shown by immunohistochemistry using a P450 2A13-specific antibody (*40*). Therefore, P450 2A13 could play important roles in the metabolic activation or detoxification of numerous procarcinogens and toxicants in air pollutants or tobacco constituents. Since P450 1A1, 2A6, and 2E1 are expressed in the human lung (*41*), they may also contribute to their metabolism. If we can quantitatively compare these expression levels in the human lung, it would be possible to determine which P450 isoform makes the major contribution.

For the *P450 2A13* gene, genetic polymorphisms (http://www.cypalleles.ki.se/cyp2a13.htm) are known. The *P450 2A13*2* allele leading to a substitution of Arg to Cys at the 257 position has been reported to decrease enzyme activities for NNK α-hydroxylation, hexamethylphosphoramide *N*-demethylation, *N,N*-dimethylaniline *N*-demethylation, 2′-methoxyacetophenone *O*-demethylation, and *N*-nitrosomethylphenylamine *N*-demethylation (*42*). The *P450 2A13*3* allele causing a frame-shift and *P450 2A13*7* allele having a stop codon at exon 2 (*43*) are predicted to produce the protein lacking enzymatic activity. Wang et al. reported that the *P450 2A13*4* allele leading to a substitution of Arg to Glu at the 101 position caused the lack of protein expression and enzyme activity (*44*). It has been reported that a single nucleotide polymorphism of 7520C > G in the 3′-untranslated region was related to decreased expression in the lung (*45*). The reported association between *P450 2A13* genetic polymorphisms and lung cancer risk is of particular interest (*46, 47*) because P450 2A13 catalyzes the metabolic activation of tobacco-specific carcinogens such as NNK. The genetic polymorphisms of *P450 2A13* might be responsible for the interindividual variability in the carcinogenicity or toxicity of naphthalene, styrene, and toluene.

In conclusion, we found that P450 2A13 can metabolize naphthalene, styrene, and toluene that are included in air pollutants and tobacco smoke. This knowledge increases our understanding of the toxicological significance of P450 2A13 expressed in the respiratory tract.

Acknowledgment. This study was supported in part by a grant from the Smoking Research Foundation in Japan. Tatsuki Fukami was supported as a Research Fellow of the Japan Society for the Promotion of Science. We thank Brent Bell for reviewing the manuscript.

Supporting Information Available: Effects of Cytochrome b_5 on chlorzoxazone 6-hydroxylation, *p*-nitrophenol 2-hydroxylation, styrene 7,8-epoxidation, and toluene methyl hydroxylation catalyzed by P450 2A6, 2A13, and 2E1 (Figure S1). This material is available free of charge via the Internet at http://pubs.acs.org.

References

(1) Fernandez-Salguero, P., Hoffman, S. M. G., Cholerton, S., Mohrenweiser, H., Raunio, H., Rautio, A., Pelkonen, O., Huang, J., Evans, W. E., Idle, J. R., and Gonzalez, F. J. (1995) A genetic polymorphism in coumarin 7-hydroxylation: Sequence of the human *CYP2A* genes and identification of variant *CYP2A6* alleles. *Am. J. Hum. Genet. 57*, 651–660.

(2) Yamano, S., Tatsuno, J., and Gonzalez, F. J. (1990) The CYP2A3 gene product catalyzes coumarin 7-hydroxylation in human liver microsomes. *Biochemistry 29*, 1322–1329.

(3) Su, T., Bao, Z., Zhang, Q. Y., Smith, T. J., Hong, J. Y., and Ding, X. (2000) Human cytochrome P450 CYP2A13: predominant expression in the respiratory tract and its high efficiency metabolic activation of a tobacco-specific carcinogen, 4-(methylnitrosamino)-1-(3-pyridyl)-1-butanone. *Cancer Res. 60*, 5074–5079.

(4) Bao, Z., He, X. Y., Ding, X., Prabhu, S., and Hong, J. Y. (2005) Metabolism of nicotine and cotinine by human cytochrome P450 2A13. *Drug Metab. Dispos. 33*, 258–261.

(5) Koskela, S., Hakkola, J., Hukkanen, J., Pelkonen, O., Sorri, M., Saranen, A., Anttila, S., Fernandez-Salguero, P., Gonzalez, F., and Raunio, H. (1999) Expression of CYP2A genes in human liver and extrahepatic tissues. *Biochem. Pharmacol. 57*, 1407–1413.

(6) Gu, J., Su, Y., Chen, Q. Y., Zhang, X., and Ding, X. (2000) Expression and biotransformation enzymes in human fetal olfactory mucosa: potential roles in developmental toxicity. *Toxicol. Appl. Pharmacol. 165*, 158–162.

(7) He, X. Y., Tang, L., Wang, S. L., Cai, Q. S., Wang, J. S., and Hong, J. Y. (2006) Efficient activation of aflatoxin B_1 by cytochrome P450 2A13, an enzyme predominantly expressed in human respiratory tract. *Int. J. Cancer 118*, 2665–2671.

(8) Fukami, T., Nakajima, M., Sakai, H., Katoh, M., and Yokoi, T. (2007) CYP2A13 metabolizes the substrates of human CYP1A2, phenacetin and theophylline. *Drug Metab. Dispos. 35*, 335–339.

(9) Nakajima, M., Ito, M., Sakai, H., Fukami, T., Katoh, M., Yamazaki, H., Kadlubar, F. F., Imaoka, S., Funae, Y., and Yokoi, T. (2006) CYP2A13 expressed in human bladder metabolically activates 4-aminobiphenyl. *Int. J. Cancer 119*, 2520–2526.

(10) Kulisch, G. P., and Vilker, V. L. (1991) Application of *Pseudomonas pulid* PpG786 containing P-450 cytochrome monooxygenase for removal of trace naphthalene concentrations. *Biotechnol. Prog. 7*, 93–98.

(11) Stucker, I., Bouyer, J., Mandereau, L., and Hemon, D. (1993) Retrospective evaluation of the exposure to polycyclic aromatic hydrocarbons: comparative evaluations with a job exposure matrix and by experts in industrial hygiene. *Int. J. Epidemiol. 22*, 5106–5112.

(12) Vuchetich, P. J., Bagchi, D., Bagchi, M., Hassoun, E. A., Tang, L., and Stohs, S. J. (1996) Naphthalene-induced oxidative stress in rats and the prospective effects of vitamine E succinate. *Free Radical Biol. Med. 21*, 577–590.

(13) Wilson, A. S., Davis, C. D., Williams, D. P., Buckpitt, A. R., Pirmohamed, M., and Park, B. K. (1996) Characterisation of the toxic metabolite. (s) of naphthalene. *Toxicology 114*, 233–242.

(14) Cho, T. M., Rose, R. L., and Hodgson, E. (2006) In vitro metabolism of naphthalene by human liver microsomal cytochrome P450 enzymes. *Drug. Metab. Dispos. 34*, 176–183.

(15) Kanekal, S., Plopper, C., Morin, D., and Buckpitt, A. (1991) Metabolism and cytotoxicity of naphthalene oxide in the isolated perfused mouse lung. *J. Pharmacol. Exp. Ther. 256*, 391–401.

(16) Buckpitt, A., Chang, A. M., Weir, A., Van Winkle, L., Duan, X., Philpot, R., and Plopper, C. (1995) Relationship of cytochrome P450 activity to Clara cell cytotoxicity. IV. Metabolism of naphthalene and naphthalene oxide in microdissected airways from mice, rats and hamsters. *Mol. Pharmacol. 47*, 74–81.

(17) IARC (1989) *Toluene. IARC Monograph on Evaluation of the Carcinogenic Risks of Chemicals to Humans 47*, 79–123, IARC, Vienna, Austria.

(18) IARC (1994) *Styrene. IARC Monograph on Evaluation of the Carcinogenic Risks of Chemicals to Humans 60*, 233–320, IARC, Vienna, Austria.

(19) Bond, J. A. (1989) Review of the toxicology of styrene. *CRC Crit. Rev. Toxicol. 19*, 227–249.

(20) Foo, S. C., Jeyaratnam, J., and Koh, D. (1990) Chronic neurobehavioral effects of toluene. *Br. J. Ind. Med. 47*, 480–484.

(21) Nakajima, T., Elovaara, E., Gonzalez, F. J., Gelboin, H. V., Raunio, H., Pelkonen, O., Vainio, H., and Aoyama, T. (1994) Styrene metabolism by cDNA-expressed human hepatic and pulmonary cytochromes P450. *Chem. Res. Toxicol. 7*, 891–896.

(22) Tassaneeyakul, W., Birkett, D. J., Edwards, J. W., Veronese, M. E., Tassaneeyakul, W., Tukey, R. H., and Miners, J. O. (1996) Human cytochrome P450 isoform specificity in the regioselective metabolism of toluene and *o*-, *m*- and *p*-xylene. *J. Pharmacol. Exp. Ther. 276*, 101–108.

(23) Nakajima, T., Wang, R-S., Elovaara, E., Gonzalez, F. J., Gelboin, H. V., Raunio, H., Pelkonen, O., Vainio, H., and Aoyama, T. (1997) Toluene metabolism by cDNA-expressed human hepatic cytochrome P450. *Biochem. Pharmacol. 53*, 271–277.

(24) Yamazaki, H., Nakamura, M., Komatsu, T., Ohyama, K., Hatanaka, N., Asahi, S., Shimada, N., Guengerich, F. P., Shimada, T., Nakajima, M., and Yokoi, T. (2002) Roles of NADPH-P450 reductase and apo- and holo-cytochrome b_5 on xenobiotic oxidations catalyzed by 12 recombinant human cytochrome P450s expressed in membranes of *Escherichia coli*. *Protein Expression Purif. 24*, 329–337.

(25) Fukami, T., Nakajima, M., Yoshida, R., Tsuchiya, Y., Fujiki, Y., Katoh, M., McLeod, H. L., and Yokoi, T. (2004) A novel polymorphism of human *CYP2A6* gene *CYP2A6*17* has an amino acid substitution (V365M) that decreases enzymatic activity in vitro and in vivo. *Clin. Pharmacol. Ther. 76*, 519–527.

(26) Yamanaka, H., Nakajima, M., Fukami, T., Sakai, H., Nakamura, A., Katoh, M., Takamiya, M., Aoki, Y., and Yokoi, T. (2005) CYP2A6 and CYP2B6 are involved in nornicotine formation from nicotine in humans: interindividual differences in these contributions. *Drug Metab. Dispos. 33*, 1811–1818.

(27) Omura, T., and Sato, R. (1964) The carbon monoxide-binding pigment of liver microsomes. *J. Biol. Chem. 239*, 2370–2378.

(28) Bradford, M. M. (1976) A rapid and sensitive method for the quantitation of microgram quantities of protein utilizing the principle of protein-dye binding. *Anal. Biochem. 72*, 248–254.

(29) Williams, C. H., Jr., and Kamin, H. (1962) Microsomal triphosphopyridine nucleotide-cytochrome c reductase of liver. *J. Biol. Chem. 237*, 587–595.

(30) Yasukochi, Y., and Masters, B. S. (1995) Some properties of detergent-solubilized NADPH-cytochrome c (cytochrome P-450) reductase purified by biospecific affinities chromatography. *J. Biol. Chem. 251*, 5337–5344.

(31) Parikh, A., Gillam, E. M., and Guengerich, F. P. (1997) Drug metabolism by *Escherichia coli* expressing human cytochromes P450. *Nat. Biotechnol. 15*, 784–788.

(32) Court, M. H., Von Moltke, L. L., Shader, R. I., and Greenblatt, D. J. (1997) Biotransformation of chlorzoxazone by hepatic microsomes from humans and ten other mammalian species. *Biopharm. Drug Dispos. 18*, 213–226.

(33) Jiang, Y., Kuo, C. L., Pernecky, S. J., and Piper, W. N. (1998) The detection of cytochrome P450 2E1 and its catalytic activity in rat testis. *Biochem. Biophys. Res. Commun. 246*, 578–583.

(34) Asikainen, A., Tarhanen, J., Poso, A., Pasanen, M., Alhava, E., and Juvonen, R. O. (2003) Predictive value of comparative molecular field analysis modeling of naphthalene inhibition of human CYP2A6 and mouse CYP2A5 enzymes. *Toxicol. in Vitro 17*, 449–455.

(35) Shield, A. J., and Sanderson, B. J. (2004) A recombinant model for assessing the role of GSTM1 in styrene-7,8-oxide toxicity and mutagenecity. *Toxicology 195*, 61–68.

(36) Laffon, B., Perez-cadahia, B., Pasaro, E., and Mendez, J. (2003) Individual sensitivity to DNA damage induced by styrene *in vitro*: influence of cytochrome P450 epoxide hydrolase and glutathione *S*-transferase genotypes. *Toxicology 186*, 131–141.

(37) Guengerich, F. P., Kim, D. H., and Iwasaki, M. (1991) Role of human cytochrome P450 2E1 in the oxidation of many low molecular weight cancer suspects. *Chem. Res. Toxicol. 4*, 168–179.

(38) Smith, B. D., Sanders, J. L., Porubsky, P. R., Lushington, G. H., Stout, C. D., and Scott, E. E. (2007) Structure of the human lung cytochrome P450 2A13. *J. Biol. Chem. 282*, 17306–17313.

(39) Sansen, S., Yano, J. K., Reynald, R. L., Schoch, G. A., Griffin, K. J., Stout, C. D., and Johnson, E. F. (2007) Adaptations for the oxidation of polycyclic aromatic hydrocarbons exhibited by the structure of human P450 1A2. *J. Biol. Chem. 282*, 14348–14355.

(40) Zhu, L. R., Thomas, P. E., Lu, G., Reuhl, K. R., Yang, G. Y., Wang, L. D., Wang, S. L., Yang, C. S., He, X. Y., and Hong, J. Y. (2006) CYP2A13 in human respiratory tissues and lung cancers: an immunohistochemical study with a new peptide-specific antibody. *Drug Metab. Dispos. 34*, 1672–1676.

(41) Shimada, T., Yamazaki, H., Mimura, M., Wakamiya, N., Ueng, Y.-F., Guengerich, F. P., and Inui, Y. (1996) Characterization of microsomal cytochrome P450 enzymes involved in the oxidation of xenobiotic chemicals in human fetal livers and adult lungs. *Drug Metab. Dispos. 24*, 515–522.

(42) Zhang, X., Su, T., Zhang, Q. Y., Gu, J., Caggana, M., Li, H., and Ding, X. (2002) Genetic polymorphisms of the human *CYP2A13* gene: identification of single-nucleotide polymorphisms and functional characterization of an Arg257Cys variant. *J. Pharmacol. Exp. Ther. 302*, 416–423.

(43) Fujieda, M., Yamazaki, H., Kiyotani, K., Muroi, A., Kunitoh, H., Dosaka-Akita, H., Sawamura, Y., and Kamataki, T. (2003) Eighteen novel polymorphisms of the *CYP2A13* gene in Japanese. *Drug Metab. Pharmacokinet. 18*, 86–90.

(44) Wang, S. L., He, X. Y., Shen, J., Wang, J. S., and Hong, J. Y. (2006) The missense genetic polymorphisms of human CYP2A13: functional significance in carcinogen activation and identification of a null allelic variant. *Toxicol. Sci. 94*, 38–45.

(45) Zhang, X., Caggana, M., Cutler, T. L., and Ding, X. (2004) Development of a real-time polymerase chain reaction-based method for the measurement of relative allelic expression and identification of CYP2A13 alleles with decreased expression in human lung. *J. Pharmacol. Exp. Ther. 311*, 373–381.

(46) Wang, H., Tan, W., Hao, B., Miao, X., Zhou, G., He, F., and Lin, D. (2003) Substantial reduction in risk of lung adenocarcinoma associated with genetic polymorphism in CYP2A13, the most activate cytochrome P450 for the metabolic activation of tobacco-specific carcinogen NNK. *Cancer Res. 63*, 8057–8061.

(47) Cauffiez, C., Lo-Guidice, J.-M., Quaranta, S., Allorge, D., Chevalier, D., Cenee, S., Hamdan, R., Lhermitte, M., Lafitte, J.-J., Libersa, C., Colombel, J.-F., Stücker, I., and Broly, F. (2004) Genetic polymorphism of the human cytochrome CYP2A13 in a French population: implication in lung cancer susceptibility. *Biochem. Biophys. Res. Commun. 317*, 662–669.

TX700325F